Review

Nano Electrocatalysts Engineering for Hydrogen Evolution Reaction by Water Splitting at High Current Density

Longlu Wang *

Posted Date: 13 May 2024

doi: 10.20944/preprints202405.0854.v1

Keywords: high current density; hydrogen evolution reaction; electrocatalyst; water splitting

Review

Nano Electrocatalysts Engineering for Hydrogen Evolution Reaction by Water Splitting at High Current Density

Bao Zang [1], Xianya Liu [1], Ghen Gu [1], Jianmei Chen [1] and Longlu Wang [1,*] and Weihao Zheng [2,*]

[1] College of Electronic and Optical Engineering & College of Flexible Electronics (Future Technology), Nanjing University of Posts and Telecommunications, Nanjing 210023, China;
[2] College of Advanced Interdisciplinary Studies & Hunan Provincial Key Laboratory of Novel Nano Optoelectronic Information Materials and Devices, National University of Defense Technology, Changsha, Hunan 410073, PR China
* Correspondence: wanglonglu@njupt.edu.cn; zhengweihao@nudt.edu.cn

Abstract: Hydrogen is now recognized as the primary alternative to fossil fuels due to its renewable, safe, high energy density and environmentally friendly properties. Efficient hydrogen production through water splitting has laid the foundation for sustainable energy technologies. However, when hydrogen production is scaled up to industrial levels, operating at high current densities introduces unique challenges. It is necessary to design advanced electrocatalysts for hydrogen evolution reaction (HER) under high current densities. This review will briefly introduce challenges posed by high current densities on electrocatalyst, including catalystic activity, mass diffusion and catalyst stability. In an attempt to address these issues, various electrocatalyst design strategies are summarized in detail. In the end, our insights into future challenges for efficient large-scale industrial hydrogen production from water splitting are presented. This review is expected to guide the rational design of efficient high current density water electrolysis electrocatalysts and promote the research progress of sustainable energy.

Keywords: high current density; hydrogen evolution reaction; electrocatalyst; water splitting

1. Introduction

Hydrogen, with its renewable, safe, high-quality energy density and environmentally friendly properties, has emerged as the top alternative to fossil fuels [1–3]. In contrast to other methods such as steam methane reforming, biomass and coal gasification for hydrogen production, water splitting for hydrogen production stands out as the most extensively adopted and developed method, especially known for its straightforward and non-polluting process [4–6]. However, the majority of HER electrocatalysts are evaluated at low current densities of 10 to 100 mA cm^{-2}, which is far from satisfactory for industrial applications [7,8]. Particularly, it is remarkable to observe the significant benefits of extending it to industrial conditions for efficient water splitting at high current densities [9–11].

Initially, the HER is an electrochemical process driven by electron transfer through current [12–14]. The efficiency of the electrolysis process increases with higher current densities, which reduces energy consumption [15–18]. Moreover, elevated current densities enhance hydrogen production efficiency, substantially boosting the volume of hydrogen produced per unit time . As a general rule, industrial-scale applications require current densities above 500 mA cm^{-2} , and high currents need to be combined with the lowest possible voltage [19–21]. For example, the U.S. Department of Energy plans to achieve 1600 mA cm^{-2} of industrial water electrolysis at 1.66 V by 2040.

Nonetheless, today's industrial application for hydrogen production by water splitting are confronted with numerous key challenges [22–24]. Firstly, the cost of catalysts remains prohibitively high: Commercially used catalysts still primarily consist of noble metals such as Pt, Ir, Ru, noted for their high cost and limited availability [25]. Thus, it's crucial to advance catalysts made from non-

 doi:10.20944/preprints202405.0854.v1

noble metals that are plentiful on Earth . Secondly, non-noble metal catalysts lack sufficient activity: At present, the performance of non-precious metal catalysts still fails to meet the standards of precious metal catalysts [26–29]. Finally, catalysts are subject to serious stability issues under high current densities at the ampere level, particularly with the problem of catalyst shedding .

Hence, the construction of non-precious metal-based electrocatalytic electrodes with enduring stability at ampere-level current densities is vital for water splitting hydrogen production technologies aimed at industrial applications. This review summarizes several electrocatalyst design strategies to address the issues of catalystic activity, mass diffusion and catalyst stability faced by non-precious metal-based electrocatalysts under industrial-scale high current densities (Figure 1).

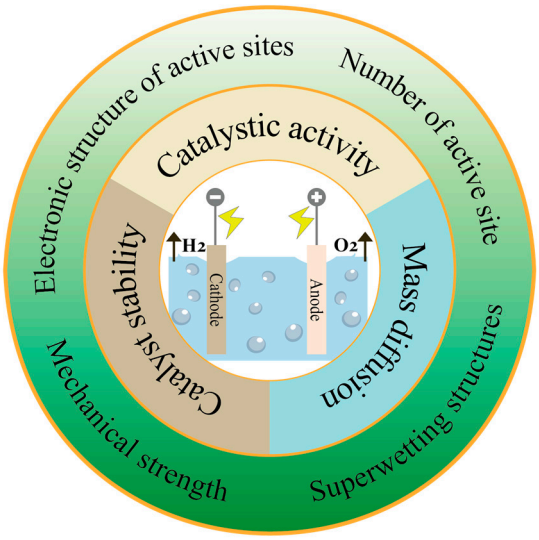

Figure 1. Challenges faced by electrocatalysts for HER under industrial high-current-density water electrolysis.

2. Challenges of Electrocatalysts Faced for HER under High Current Density

The HER during water splitting is composed of several key steps, including the adsorption of reactants at the active sites, electron transfer from the support to the catalyst, and detachment of gas bubbles [30–32]. Moreover, high current densities can induce transformations in structure and composition, thereby reducing the stability of electrocatalysts . In this regard, to enhance the performance of electrocatalysts under high current densities, it is crucial to deeply analyze this key challenges.

From the perspective of electrochemical process, conductivity is one of the intrinsic factors affecting the activity of catalysts [33–35]. At high current densities, the multi-electrons electrochemical reaction is violent and fast, resulting in the active sites on the catalyst surface being easily occupied and allowing rapid charge consumption [36,37]. If the electron transfer is not fast enough, the charge consumption will exceed the charge supply, affecting the efficiency of the catalytic reaction . The rate of charge transfer depends on the conductivity and interfacial resistance of the support-catalyst interface . The conductivity is determined by several factors. Firstly, the crystal structure of the support-catalyst interface can affect the electron transfer and conduction . For example, defects or impurities in the crystal structure can introduce additional energy levels and affect the electron conductivity [38]. Secondly, the surface morphology can affect the electron transport on the support-catalyst interface [39]. Nanostructures with a high specific surface area and a large number of active sites may provide more electron transport channels and thus increase conductivity [40–42]. Finally, when large Fermi energy level difference between the conductor support and the semiconductor catalyst occur , the Schottky barrier may form at the support-catalyst interface and electrons cannot be transferred efficiently from the electron-rich to the electron-negative region, making the charge transfer at the interface hindered . As a result, an additional overpotential

 doi:10.20944/preprints202405.0854.v1

is required to overcome the energy barrier, which deteriorates the electrocatalytic performance at high current densities.

According to Faraday's law, the rate of hydrogen production is directly proportional to the current density [43–46]. Therefore, for HER at high current densities, the bubble detachment performance has always been an important factor to consider . Similar to electron transfer, when bubble detachment is hindered, the blocked bubbles will limit the catalytic performance of the electrocatalyst [47,48]. Specifically, bubbles adhere to the electrode surface and accumulate at the contact surface between the electrocatalyst and the electrolyte, severely restricting the mass transfer of the liquid and massively blocking the active sites on the electrocatalyst . Since the bubbles cover the electrode surface, the actual surface area of the electrocatalyst involved in the reaction is reduced, decreasing the efficiency of the electrocatalytic reaction [49–51]. Moreover, this large-scale coverage undoubtedly leads to poor contact between the electrolyte and the electrode and increases the internal resistance of the system [52,53].

When conducting water splitting for hydrogen production at high current densities, electrocatalysts face stability challenges categorized into chemical and mechanical stability. In terms of chemical stability, the conditions of high current densities may lead to changes in the crystal structure, surface morphology, and pore structure of the catalyst, thereby diminishing the catalyst's stability [54–56]. Moreover, the substantial electron transfer occurring under high current densities accelerates the catalyst's reconstruction process, imposing more severe effects on the catalyst. Regarding mechanical stability, the significant impact of electrochemical shear forces, along with the thermal effects encountered at high current densities, may cause insufficient interfacial adhesion between the catalyst and the support, making the catalyst prone to detachment during the reaction . Furthermore, the heat generated during the reaction raises the electrode's temperature, which not only compromises the catalyst's chemical stability but may also change the material's physical properties, like causing swelling or softening, further weakening the bond between the catalyst and the support [57,58].

The above-mentioned series of problems cause the hydrogen production performance of electrocatalysts at high current density to be far from ideal. Consequently, to enhance hydrogen production efficiency under high current densities, additional advancements in catalyst design are required.

3. Design Strategies of Electrocatalysts for HER under High Current Densities

As highlighted above, catalystic activity, mass diffusion, and catalyst stability represent the three principal challenges in achieving water splitting at high current densities. To surmount these obstacles, it is imperative to judiciously design water-splitting electrocatalysts that simultaneously enhance activity and stability. Consequently, this section delves into electrocatalyst design strategies in terms of electronic structure of active sites, number of active site, superwetting structures and mechanical strength. These strategies are critical for optimizing the catalysts' performance by addressing the specific challenges posed at high current densities.

3.1. Tuning Electronic Structure and Crystal Phase of the Catalyst for Enhancing Intrinsic Activity

For high-performance HER electrocatalysts operating at high current densities, possessing high intrinsic activity and excellent electrical conductivity are key to their performance. Achieving these characteristics requires the precise modulation of the electronic structure, which not only significantly enhances the intrinsic activity of the catalysts, but also improves its conductivity, thereby greatly increasing the efficiency and stability of the water electrolysis process under high current density conditions. Strategies for optimizing the electronic structure and crystal phase of the catalyst are diverse, including but not limited to defect engineering, alloying, heterostructure, and amorphization (Figure 2a-b).

By meticulously designing defects in the electrocatalysts, such as through heteroatom doping, vacancy engineering, and dislocation modulation, the electronic structure can be effectively tuned and the adsorption energy of reaction intermediates optimized [59]. Heteroatom doping strategies

 doi:10.20944/preprints202405.0854.v1

entail incorporating non-intrinsic heteroatoms into the catalyst's lattice. Specifically, this approach can modify the material's electronic environment by either replacing original lattice positions or embedding into lattice interstices.

Precious metal atoms, such as Pt and Ru, are widely employed in doping strategies because of their excellent catalytic performance. However, the high cost of precious metals limits its feasibility in large-scale applications. In response, there's a growing interest within the scientific community to identify more economically feasible alternatives among transition metals, which have similarly demonstrated remarkable capabilities in electronic structure modulation and electron transfer enhancement. For example, Zhang et al. successfully synthesized a Ce-doped CoP/Ni_3P composite through a combination of corrosion, electrodeposition, and phosphorization calcination methods . By doping Ce, they modulated the electronic structure of the CoP/Ni_3P electrocatalyst to enhance the electron transfer process (Figure 2c). Ce doping effectively redistributed charge and adjusted the d-band center, which not only accelerated the dissociation step of H_2O but also promoted the kinetics of alkaline water splitting at high current densities (Figure 2d). This adjustment of the electronic structure resulted in an overpotential of just 225 mV at a high current density of 1000 mA cm^{-2} (Figure 2e), with the ability to operate stably in alkaline electrolytes for 200 hours, demonstrating excellent catalytic activity and stability. Furthermore, the doping of non-metal elements is an effective approach to enhance the performance of electrocatalysts. Nitrogen-doped carbon is widely used in the preparation process of electrocatalysts, certificating the profound impact of non-metal doping. Moreover, Wang et al. reported the synergistic preparation of Ru/P-NiMoO4@NF with P doping and Ru doping, whose multi-channel hollow structure facilitates the rapid transfer of charges. The results show that Ru/P-NiMoO4@NF demonstrates excellent HER activity across both alkaline simulated seawater and natural alkaline solutions.

In addition to heteroatom doping, the introduction of vacancies has also been broadly utilized to modify the electronic structure of electrocatalysts. Interestingly, the relationship between different concentrations of vacancies and HER activity is inherently linked. For example, Sun and his team used Bi_2O_3 nanosheets as a model system to investigate the effect of different concentrations of oxygen vacancies (V_o) created by plasma irradiation on HER performance. Initially, the introduction of V_o was found to improve charge transfer and provide more active sites for hydrogen adsorption, thereby enhancing HER activity. This enhancement is attributed to the changes in the catalyst's electronic structure and surface chemistry due to the presence of V_o (Figure 2f-h). However, the study also discovered a critical threshold for V_o concentration. Beyond this saturation point, further increases in V_o concentration led to a significant decline in HER activity. These findings suggest that there is an optimal V_o concentration that maximizes HER performance by balancing the benefits of increased active sites and enhanced charge transfer against the negative effects of excessive V_o.

Moreover, in the realm of defect engineering for electrocatalysis, the strategic incorporation of dislocation networks emerges as a critical innovation for enhancing the efficacy of HER. Yang's study highlighted that a original fabrication technique leveraging millisecond laser direct-write synthesis within a liquid nitrogen environment was utilized to craft PtNi alloy nanoparticles adorned with intricate dislocation networks on nickel foam substrates. This methodologically advanced design of dislocation networks serves a dual-purpose. Firstly, it greatly facilitates the basic process of alkaline HER by introducing large tensile-compressive coupling strains. From the kinetic point of view, HSD-PtNi has a much lower water dissociation barrier (ΔG_B, 0.73 eV) than that of PtNi and Pt (Figure 2i). Secondly, the electron density of Ni atoms experiencing the maximum tensile strain is significantly reduced, resulting in stronger electronic interactions between the H_2O molecule and the Ni sites (Figure 2j). This enhancement strengthens the intrinsic activity of a range of surface active sites. Furthermore, it robustly secures the surface dislocations against the challenges posed by high current densities, ensuring an unparalleled level of stability and performance under demanding conditions. The results show that HSD-PtNi has significantly lower overpotentials at high current densities than PtNi/NF and Pt/C/NF, and only requires a very low overpotential of 63 mV to achieve an ultra-high current density of 1 A cm^{-2} (Figure 2k). In addition, Zhou et al. also considered the potential of employing this technique for the production of electrocatalysts. Contrary to the aforementioned

 doi:10.20944/preprints202405.0854.v1

research, this group aimed to replace platinum-based catalysts with palladium-based (Pd-based) ones, and they successfully prepared D-$Ni_{3.5}Pd$/NF characterized by a high density of dislocations. These dislocations led to the reduction of the hydrogen adsorption energy of the Pd site and the enhancement of water dissociation of Ni sites, significantly improving the intrinsic activity of this electrocatalyst. Impressively, this catalyst requires only a 352 mV overpotential to achieve a current density of 1000 mA cm^{-2}, greatly advancing HER performance.

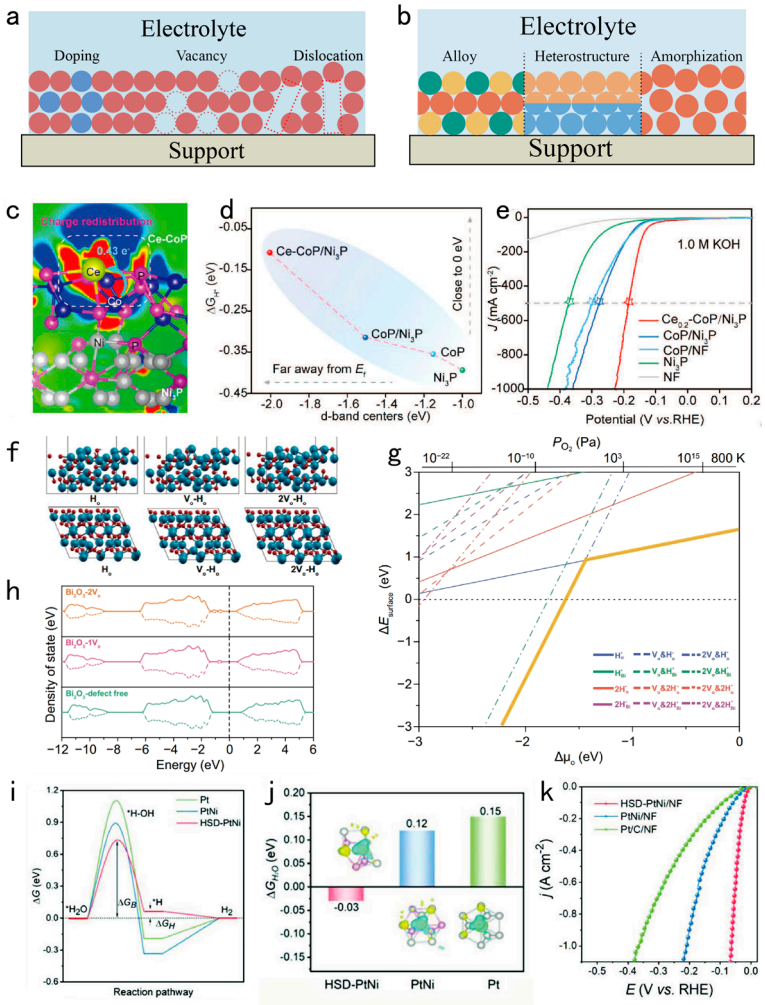

Figure 2. Strategies for dealing with rapid electron transfer at high current densities. **(a)** Defect engineering (including heteroatom doping, vacancy engineering and dislocation modulation). **(b)** Alloying, heterostructure and amorphization. **(c)** Differential charge density 2D slice of the Ce-CoP/Ni_3P. **(d)** The tailoring relationship between ΔG_{H^*} and d-band centers (ε_d). **(e)** J–V curves of $Ce_{0.2}$-CoP/Ni_3P@NF, CoP/Ni_3P@NF, CoP/NF, Ni_3P@NF, and bare NF. Adapted with permission from [60], Copyright 2022 Wiley-VCH GmbH. **(f)** hydrogen atom adsorbed Bi_2O_3 (010) surface models in defect-free state and with one or two oxygen vacancy incorporated. **(g)** The calculated relative surface energies as functions of the chemical potential of oxygen ($\Delta_{\mu O}$). **(h)** the spin-polarized electronic density of states of Bi_2O_3 surfaces with different oxygen vacancies coverage. Adapted with permission from [61], Copyright 2022 Springer Nature. **(i)** Gibbs free energy diagram of HER on (111) plane of HSD-PtNi, PtNi, and Pt. **(j)** Comparisons of the derived adsorption Gibbs free energies of H_2O on HSD-PtNi, PtNi, and Pt. **(k)** HER linear sweep voltammetric (LSV) curves with iR compensation. Adapted with permission from [62], Copyright 2022 Wiley-VCH GmbH.

In addition to defect engineering, strategies such as alloying, heterostructure and amorphization have also shone in the direction of facilitating charge transfer, and are considered to be powerful tools for the electronic structure modulation of electrocatalysts, laying a solid foundation for the achievement of unparalleled high current density hydrogen evolution efficiencies.

 doi:10.20944/preprints202405.0854.v1

Alloying is considered to be an efficient way to modulate electronic structure and enhance electrical conductivity, offering a cost-effective solution by alloying noble metals with transition metals. This synergistic effect not only alleviates the high cost of precious metal catalysts, but also facilitates electron transfer, tunes the Fermi energy levels, and enhances the intrinsic activity of the catalysts. Li et al. obtained CoPt-PtSA/NDPCF by incorporating Pt nanocrystals with the ZIF-67 precursor, which was further calcined at high temperatures. This structure displayed excellent homogeneity and dispersion , facilitating the improvement of the contact efficiency of the reactive active sites (Figure 3a). Furthermore, the active sites on the surface were optimized by adjusting the ratios and nanostructures of Pt and Co. CoPt-PtSA/NDPCF exhibited lower overpotentials and higher current densities than that of the commercial 10% Pt/C catalysts, suggesting superior hydrogen production performances under both alkaline and acidic conditions. With the continuous advancement in alloy research, several metal alloys have emerged and evolved over time. High-entropy alloys (HEAs) have been introduced as a novel class of alloy materials. HEAs, composed of five or more metal elements mixed, exhibit unique chemical and physical properties due to their solid-solution phases. Zhao et al. developed a nanoporous NiCoFeMoMn high-entropy alloy through a one-step dealloying process. Furthermore, they also constructed np-HEA models for SA and un-SA. The Gibbs free energies of hydrogen adsorption were calculated for all possible active sites on the surface of the material, as shown in Figure 3b. It is obvious that SA in np-HEA plays a crucial role in the hydrogen adsorption properties. The alloy shows excellent HER properties in electrolytic water tests. It achieves a current density of 1000 mA cm^{-2} at an overpotential of only 150 mV in a 1 M KOH solution (Figure 3c) and shows a Tafel slope as low as 29 mV dec^{-1}.

Heterostructures further brighten the way to optimize electronic structures and facilitate charge transfer. By cleverly combining different materials, the heterostructures provide the fundamental basis for improved water dissociation and hydrogen adsorption, which greatly enhances the catalytic efficiency under high current density condition. For instance, Zhou et al. selected porous interlaced Co_2N nanosheets and Fe_2P nanoparticles to construct an array of Fe_2P/Co_2N heterostructures. The surface of this heterostructure is abundant with Fe sites, and DFT calculations show that the interfacial interaction between Fe_2P and Co_2N can increase the H* binding energy (ΔG_{H^*}) on the Fe sites, thus improving the HER performance of the catalyst. Li's team electrodeposited MnCo layer on the prepared NiSe samples, and the added MnCo layer helps to roughen the NiSe surface (Figure 3d-e). Interestingly, the deposition of MnCo on NiSe results in a decrease in the electron density around the Ni and Se atoms. This indicates that electron transfer occurs between two materials with different electronegativities, forming a heterogeneous structure, which in turn improves the HER efficiency of the catalyst. Additionally, the Rct values of MnCo/NiSe from the Nyquist plots show a significant decrease (Figure 3f), suggesting that the electrical conductivity of MnCo/NiSe is higher than that of NiSe, which is more conducive to charge transfer.

Amorphization introduces disorder in the crystal matrix, which reveals a large number of active sites and alters the electronic properties in favor of HER. This disorder strengthens the adsorption energy regulation and accessibility of the reaction products, greatly increasing the intrinsic activity of the catalysts. For instance, Hu's team prepared amorphous Mo-doped $NiS_{0.5}Se_{0.5}$ nanosheets (Am-Mo-$NiS_{0.5}Se_{0.5}$) and uniformly wrapped them on nanorods. The formation of Am-Mo-$NiS_{0.5}Se_{0.5}$ composites resulted in a greater number of active sites, and the amorphous structure altered the local electronic structure of the active sites, thus enhancing the intrinsic activity. consequently increasing the intrinsic activity. Specifically, X-ray photoelectron spectroscopy (XPS) patterns visually demonstrate the decrease of electrons around Mo atoms and the accumulation of electrons around Ni atoms in the amorphous structure, indicating that the electron distribution of Am-Mo-$NiS_{0.5}Se_{0.5}$ has been modified, which affects its electronic structure. Meanwhile DFT theoretical calculations also show that Am-Mo-$NiS_{0.5}Se_{0.5}$ has no obvious indirect band gap, which confers its excellent performance (Figure 3g-h). It only needs overpotentials of 209 for HER at 1000 mA cm^{-2} (Figure 3i), which demonstrates a hydrogen production performance that is superior to that of crystalline structures.

Preprints.org (www.preprints.org) | NOT PEER-REVIEWED | Posted: 13 May 2024 doi:10.20944/preprints202405.0854.v1

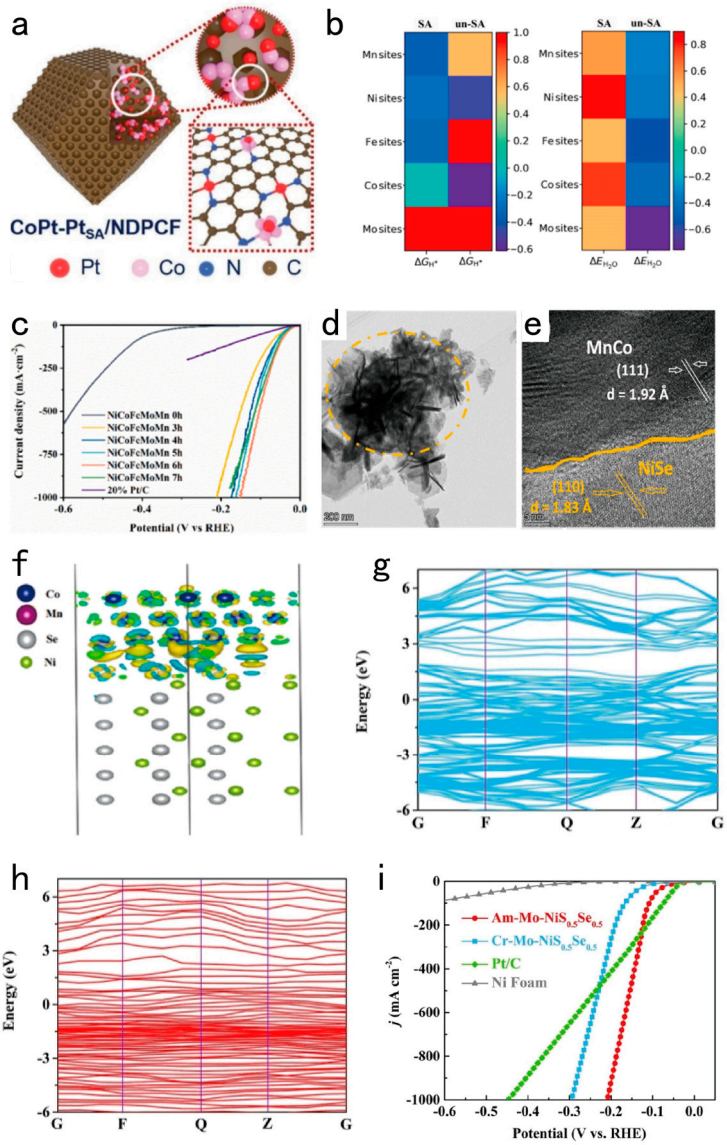

Figure 3. (a) The bimetallic CoPt-alloy nanocrystals and PtSA were confined inside the NDPCF. Adapted with permission from [63], Copyright 2022 Wiley-VCH GmbH. **(b)** The colored ΔG_{H^*} and ΔE_{H2O} comparisons of all possible active sites on regions of elemental segregation and other regions of high-entropy alloy models; the pure red area means this site is not easy to be adsorbed. **(c)** HER polarization curves for nanoporous NiCoFeMoMn and commercially available Pt/C in 1 M KOH solution. Adapted with permission from [64], Copyright 2022 Elsevier. **(d)** TEM and **(e)** HRTEM images of MnCo/NiSe electrode. **(f)** Electron density redistribution of the interface made by MnCo and NiSe. Adapted with permission from [65], Copyright 2022 Elsevier. The band structure of the **(g)** Cr-Mo-$NiS_{0.5}Se_{0.5}$ and **(h)** Am-Mo-$NiS_{0.5}Se_{0.5}$. **(i)** HER polarization curves. Adapted with permission from [66], Copyright 2022 Wiley-VCH GmbH.

3.2. Designing the Interface of the Electrocatalysts for Exposing Large Number of Active Sites

Since the overall activity of an electrocatalyst also depends on the number of its active sites, the interface of the electrocatalyst should be carefully designed to expose a large number of active sites (Figure 4a). By optimizing the interfaces between the materials in the electrocatalyst and other materials, the electron transport efficiency can be improved. For example, Wang et al. developed a non-precious Ni_2P@Cu_3P heterostructure constructed by in-situ phase conversion for electrochemical HER. Interestingly, this 3D nanowire array structure provide the large specific active surface area for the fast charge/ mass transport to accelerate the HER dynamics. Results showed that Ni_2P@Cu_3P displayed superior HER activity compared to pure Ni_2P and Cu_3P (Figure 4b). Furthermore, DFT

 doi:10.20944/preprints202405.0854.v1

calculations revealed that $Ni_2P@Cu_3P$ has more moderate free energies to promote alkaline HER, a result that confirms its effective modulation in the active site (Figure 4c). In addition, Zang et al. considered the possibility of promoting unidirectional electron transfer by means of a built-in electric field to ensure electron enrichment. The presence of a heterojunction between Ru nanoclusters and P,O-NiFe LDH/NF (as shown in Figure 4d) has been verified, serving as a catalyst for enhanced electron transfer during electrocatalysis. Additionally, the interaction between the metallic Ru clusters and the P,O-NiFe LDH leads to the creation of an intrinsic electric field, stemming from disparities in their respective Fermi levels. This allows for a seamless flow of electrons from the P,O-NiFe LDH to the Ru nanoclusters, as depicted in Figure 4e. It is worth noting that the process of water splitting achieves the industrially significant current density of 100 mA cm^{-2} at potentials of 1.584 V when conducted at temperatures of 85 ˚C (Figure 4f). Furthermore, the electrochemical durability testing of Ru NCs/P,O-NiFe LDH/NF showed almost no decay (Figure 4g), suggesting the excellent potential application prospects.

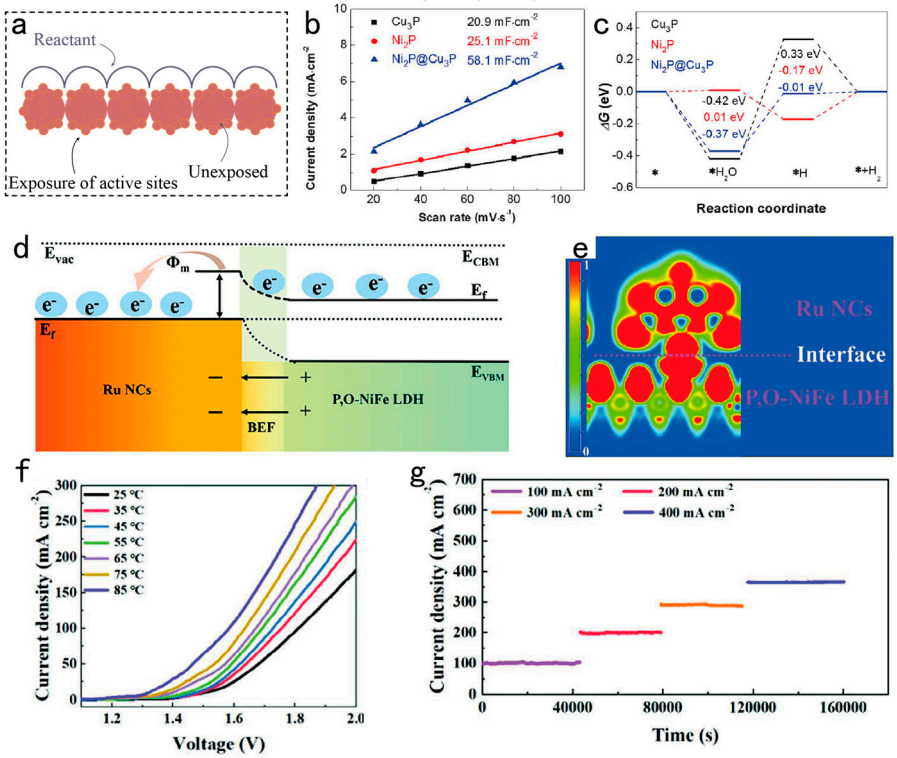

Figure 4. (a) Schematics showing exposure of active sites. **(b)** The double-layer capacitance of Ni_2P, Cu_3P and $Ni_2P@Cu_3P$. **(c)** The free energy diagrams of H_2O and H adsorbing. Adapted with permission from [67], Copyright 2023 Elsevier. **(d)** Schematic drawing of electron redistribution in Ru NCs/P,O-NiFe LDH/NF. **(e)** Differential charge density of the Ru NCs/P,O-NiFe LDH/NF, The iso-values of 0 and 1 imply low and high electron localization, respectively. **(f)** LSV curves of Ru NCs/P,O-NiFe LDH/NF for overall water splitting of the simulated seawater at different temperatures. **(g)** Chronoamperometry curves for simulated seawater at large current at 65 ˚C. Adapted with permission from [68], Copyright 2023 Wiley-VCH GmbH.

3.3. Designing Superwetting Porous Structure for Accelerating Bubble Detachment

At high current densities, abundant bubbles that are unable to detach will undoubtedly block the exposure of catalyst active sites, which seriously affects the mass transfer of the system. How to promote the rapid detachment of bubbles from the electrocatalyst remains a key issue. This review explores this issue from the perspective of catalyst structure. Thus, nanoarray configuration and porous structure are two structures worth discussing (Figure 5a).

 doi:10.20944/preprints202405.0854.v1

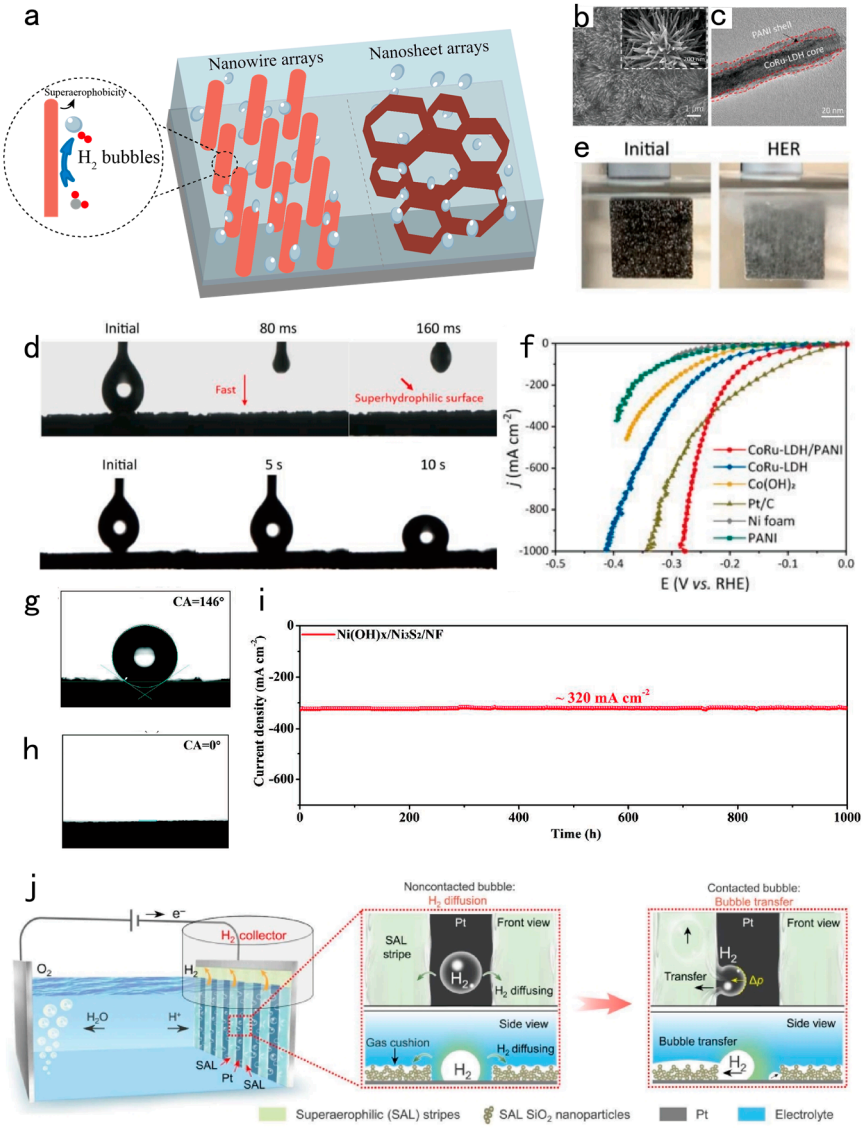

Figure 5. (a) Physical modals of the morphology engineering such as nanowire arrays and nanosheet arrays to solve the problem of bubble detachment under high current density. **(b)** SEM and **(c)** TEM images of CoRu-LDH/PANI. **(d)** Contact angle measurements of CoRu-LDH/PANI and Pt/C. **(e)** The release of H2 bubbles on CoRu-LDH/PANI. **(f)** Polarization curves based on geometric area in 1 M KOH. Adapted with permission from [69], Copyright 2022 Elsevier. **(g-h)** Contact angles of Ni_3S_2 and $Ni(OH)_x/Ni_3S_2$. **(i)** Chronopotentiometry curve of the $Ni(OH)x/Ni_3S_2/NF$ recorded at ≈320 mA cm^{-2} for 1000 h. Adapted with permission from [70], Copyright 2022 Wiley-VCH GmbH. **(j)** Schematic of the SAL/flat Pt electrode with enhanced mass transfer. Adapted with permission from [71], Copyright 2023 The American Association for the Advancement of Science.

To begin with, the nanowire arrays own unique surface properties such as high surface area and high aspect ratio, which can significantly affect the flow characteristics of the electrolyte and accelerate the penetration of the electrolyte. For instance, Yin et al. destroyed the smooth morphology of the nanoneedle structure by calcination at high temperature, which strengthened the surface wettability of the catalyst and effectively promoted the release of gas bubbles. Liu's group reported a polyaniline (PANI)-coated CoRu-LDH (CoRu-LDH/PANI) nanowire array electrocatalyst. The nanowire array itself greatly decreases the attachment time of gas bubbles on the catalyst surface by relying on its highly oriented surface structure. After coating coarse PANI onto nanowires by chemical polymerization (Figure 5b), the catalyst's ability to promote bubble detachment was dramatically improved. On the one hand, the coarse PANI brought micro- and nano-scale roughness

 doi:10.20944/preprints202405.0854.v1

to CoRu-LDH (Figure 5c), which increased the surface area of the electrocatalyst and provided more water molecule adsorption sites to facilitate the formation of water film. On the other hand, the amine-rich PANI strengthens the interface between CoRu-LDH and PANI, which contributes a superhydrophilic surface for the electrocatalyst and promotes rapid electrolyte transport and efficient desorption of gas bubbles ,as shown in Figure 5d. Moreover, only a minimal amount of bubble adhesion occurs on its surface (Figure 5e), which effectively prevents the clogging of active sites to some extent. In addition, the CoRu-LDH/PANI exhibits excellent hydrogen production performance, achieving a high current density of 1000 mA cm^{-2} at a low overpotential of just 275 mV (Figure 5f). Furthermore, nanosheet arrays are one of the most advanced non-noble metal electrocatalysts due to their superhydrophilicity, microporous nature and self-supporting structure. For example, Xin et al. possessed a self-supported microporous $Ni(OH)_x/Ni_3S_2$ heterostructure electrocatalyst through an electrochemical process. As shown in Figure 5g-h, the contact angle of $Ni(OH)_x/Ni_3S_2$ is 0°, showing that $Ni(OH)_x/Ni_3S_2$ exhibits obvious superhydrophilicity compared with the hydrophobic Ni_3S_2 electrode. Additionally, the Ni(OH)x/Ni_3S_2/NF catalyst demonstrated long-term stability for more than 1000 h (Figure 5i).

While the above series of electrocatalysts are excellent in promoting bubble detachment, the released bubbles tend to be disordered, and few studies have reported how to regulate the departure of the detached bubbles from the electrolyte. To address this issue, Jiang's team reported a superaerophilic/superaerophobic (SAL/SAB) synergistic electrode where bubbles are generated in the electrocatalytic region of the SAB (Figure 5j). the air cushion on the SAL stripes acts like a sky bridge, providing a fast path for the bubbles to leave the reaction system directly. When the bubbles contact the SAL stripes, they are transported to the external surface in a very short period of time, as if they were sitting in a car propelled by Laplace pressure.

Obviously, porous structure re more likely to promote bubble detachment. Yuan's team prepared multidimensional nanoporous interpenetrating-phase FeNiZn alloy and $FeNi_3$ intermetallic heterostructure on NiFe foam for water splitting. As shown in Figure 6a, it can be found that several second-order pores of FeNiZn/ $FeNi_3$@NiFe sample. Furthermore, FeNiZn/FeNi3@NiFe depicts exceptional bifunctional activities for water splitting with extremely low overpotentials toward HER as well as the robust durability during the 400 h testing in alkaline solution (Figure 6b).

Considering to the smaller bubble sizes implied that the bubbles had a shorter residence time at the reaction interface, which improved the detachment efficiency of the bubbles. Tang et al. presented a vital microscopic bubble/precipitate traffic system for robust anti-precipitation seawater reduction. Attributed to its unusual 3D H_2-evolving architecture, NCP/PC brings vital benefits that boost electrocatalysis efficiency, facilitate H_2 gas release traffic and grant itself superb anti-precipitation ability (Figure 6c). Noticeably, only the surface of NCP/PC is clean as before testing after the long-period of electrolysis, while other five NCP-based cathodes are covered with thick and dense Mg^{2+}/Ca^{2+} precipitates as displayed in Figure 6d-e, showing that only the NCP/PC possesses the strong anti-precipitation ability. Moreover, Such long-term seawater electrolysis durability is even better than the most advanced nature seawater electrolyzer that operated at the current density of 500 mA cm^{-2} for 100 h (Figure 6f).

 doi:10.20944/preprints202405.0854.v1

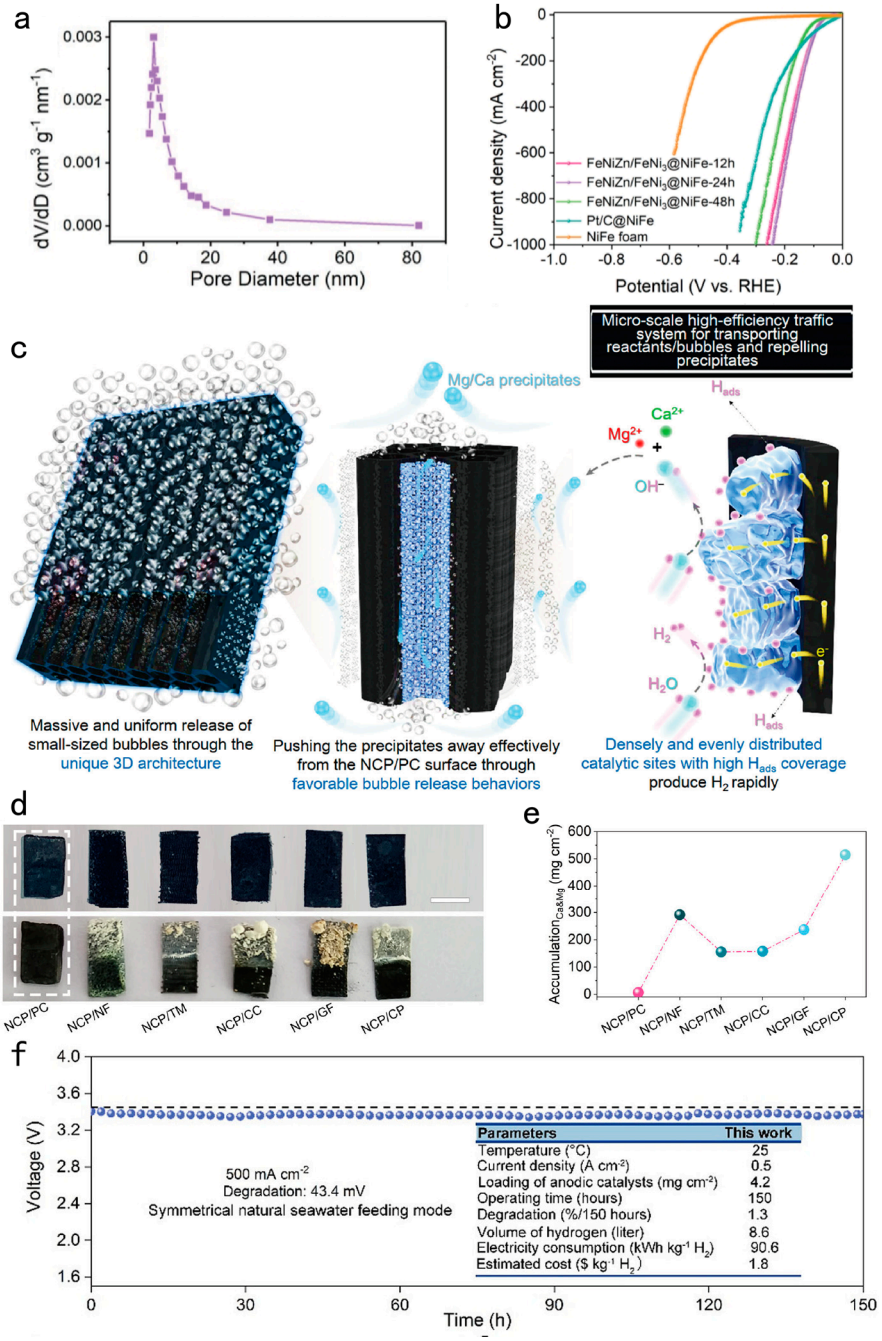

Figure 6. (a) BJH pore size distribution curve of the FeNiZn/FeNi3@NiFe sample. **(b)** LSV curves of FeNiZn/FeNi3@NiFe samples, Pt/C@NiFe, and NiFe foam in 1.0 M KOH solution at the scan rate of 5 mV s^{-1}. Adapted with permission from [72], Copyright 2023 The Author(s). **(c)** Schematic diagrams of densely and evenly distributed catalytic sites with high H_{ads} coverage produce H_2 rapidly. **(d)** Pictures of various cathodes after the 10 h of eNSR. Scale bar: 0.5 cm. **(e)** $A_{Ca\&Mg}$ values for various cathodes after the long-term eNSR testing. **(f)** Long-term stability of NCP/PC || DSA under a fixed j of 500 mA cm^{-2}. Adapted with permission from [73], Copyright 2024 The Author(s).

3.4. Modulating Surface/Interface for Enhancing the Mechanical Strength

It is well known that the surface reconstruction process of electrocatalysts is essentially a chemical reaction. Therefore, it is particularly significant to observe the reconstruction process under electrochemical conditions. A great deal of research results show that the original catalyst experiences dynamic reconstruction and generates real active sites during the reaction process, which optimizes the adsorption, activation and desorption behaviors during the catalytic process to a certain extent,

 doi:10.20944/preprints202405.0854.v1

and thus boosts the HER performance of the electrocatalysts. This type of electrocatalyst before reconstruction is called "pre-catalyst". Therefore, it is necessary to artificially intervene to adjust the reconstruction process of pre-catalysts to obtain more active sites. This review summarizes effective modulation strategies to promote the surface reconstruction process to augment the HER activity. The modulation strategies can be classified into electrochemical activation, redeposition of dissolved materials and ionic modulation of the reconstruction(Figure 7a-b).

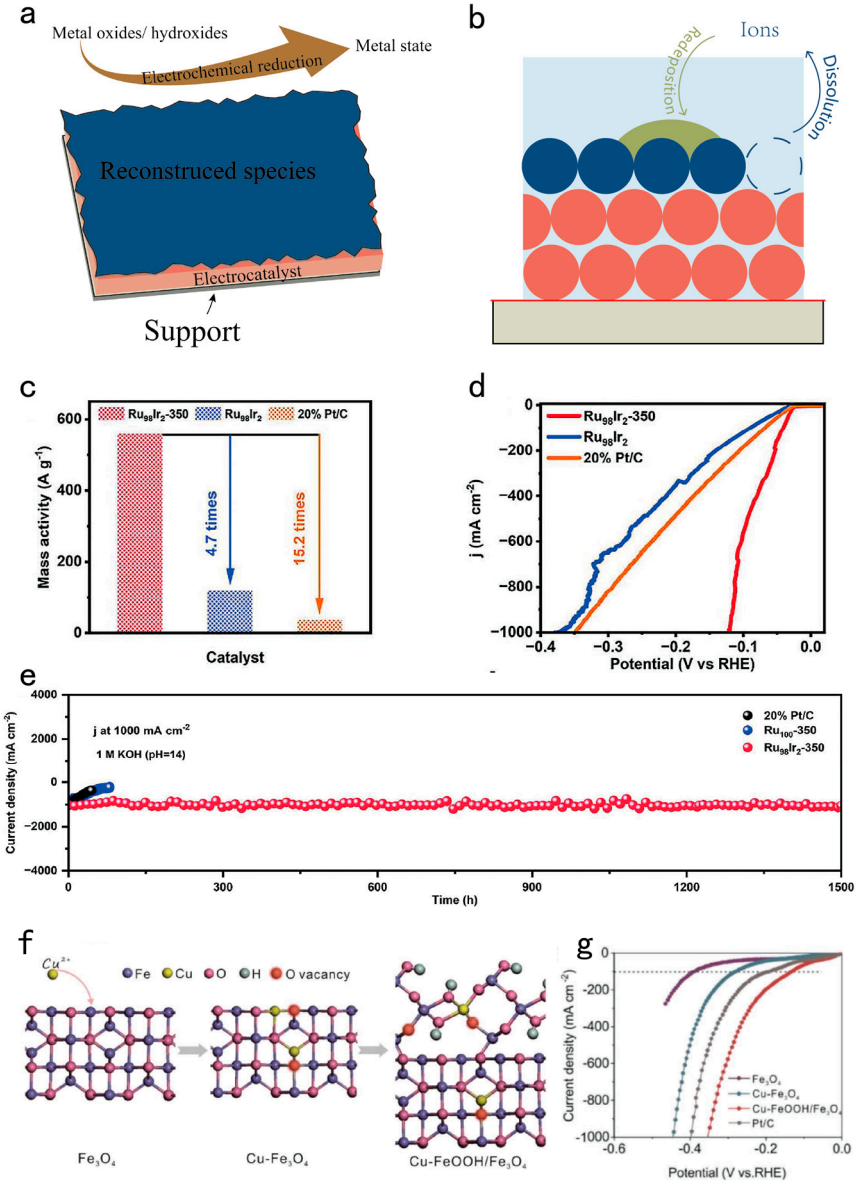

Figure 7. Schematics show key aspects for the enhancement of chemical and mechanical stability of electrocatalysts. Strategies such as **(a)** electrochemical reduction and **(b)** redeposition of dissolved materials and ionic modulation of the reconstruction to enhance the chemical stability. **(c)** Mass activity value at an overpotential of 100 mV. **(d)** LSV curves of the as-synthesized $Ru_{98}Ir_2$-350, $Ru_{98}Ir_2$ samples, and commercial Pt/C catalyst. **(e)** i-t continuous durability of $Ru_{98}Ir_2$-350, Ru_{100}, and commercial Pt/C at 1000 mA cm^{-2}. Adapted with permission from [74], Copyright 2023 The Authors. Advanced Science published by Wiley-VCH GmbH. **(f)** Schematic diagram of the structural transformation at an atomic level. **(g)** The iR-corrected LSVs of the Cu-FeOOH/Fe_3O_4 catalyst in 1 M KOH. Adapted with permission from [75], Copyright 2022 The Authors. Advanced Energy Materials published by Wiley-VCH GmbH.

 doi:10.20944/preprints202405.0854.v1

In some situations, electrochemical activation can prompt the formation of new active phases on the catalyst surface, which may have superior HER properties to the original material. Through appropriate electrochemical treatment, thin layers of metal hydrides or oxides can be formed on the catalyst surface, and these specific phases may be more active for HER reactions. For example, Lu et al. used the reducing power of sodium borohydride ($NaBH_4$) to co-reduce Ru^{3+} and Ir^{3+} in metal salts in situ to $Ru_{98}Ir_2$, which in turn could be oxidized to obtain Ir-doped partially oxidized Ru metallic aerogels. Compared to Pt/C, $Ru_{98}Ir_2$-350 delivers a higher mass activity value, as shown in Figure 7c. Notably, the $Ru_{98}Ir_2$-350 sample delivered a superior catalytic activity at current densities of 1000 mA cm^{-2}, only requiring overpotentials of 121 mV (Figure 7d). In addition, the $Ru_{98}Ir_2$-350 demonstrated excellent CV stability at 1000 mA cm^{-2}, which is illustrated in Figure 7e.

For surface reconstruction of cathode materials, the redeposition of dissolved species back to the catalyst surface has aroused much attentions. High oxidation/reduction potentials and corrosive electrolytes lead to elements dissolving and reacting with the electrolyte, and the leached components will be deposited back to the catalyst surface, resulting in a dynamically reconstructed surface with high performance and stability. For instance, Yang et al. induced abundant defects and unsaturated sites via incorporating an amorphous structure on the surface of a catalyst to enhanced HER activity. Schematic diagram of crystal structure transform at an atomic level showed that the atomic radius of Cu is close to Fe, which makes it easier to substitute Fe atoms by Cu atoms and suggests the leaching of Fe and Cu species during the formation of the CuFeOOH/Fe_3O_4 catalyst (Figure 7f). Significantly, the Cu-FeOOH/Fe_3O_4 catalyst achieves the best HER activity in 1 M KOH since it features the ultra-low overpotential of 285 mV at the current density of -500 mA cm^{-2} (Figure 7g).

For high current density electrolytic hydrogen evolution, electrocatalysts are exposed to more corrosive electrolytes, higher reaction temperatures, and higher current densities, which inevitably induce deactivation and detachment of catalytic substances from the electrocatalysts. Therefore, the designed electrocatalysts should have excellent mechanical stability in addition to high activity. Self-supported electrocatalysts are outstanding in high current density due to their unique structural design. The following discussion presents the research progress of self-supported electrocatalysts in terms of self-supported substrates and nanostructured catalysts.

Selecting an appropriate substrate is crucial for the preparation of self-supported electrocatalysts. Metal-based catalysts, such as metal foams and metal meshes, have attracted widespread attention (Figure 8a). Besides nickel foam, other metal-based foams like iron foam (IF), cobalt foam (CF), and copper foam (CFM) have also been extensively studied.

Apart from the metallic foams mentioned above, other non-metallic substrates are being explored. For example, insulating materials such as flexible glass fibers, paper or cloth, and sponges (Figure 8b) as substrates are promising materials. Hao et al. realized the significance of flexible materials in realizing the long-term stability of electrocatalysts. With the help of precision instruments, they achieved the deposition of 3D dandelion gown-like Fe_1-Ni_2P onto a flexible glass fiber substrate. The electrocatalyst prepared not only possesses advantages such as corrosion resistance and good elasticity, but also exhibits a loose and porous characteristic, which contribute to the enhancement of hydrogen evolution of the electrocatalyst at high current densities. Notably, the research team also extended its application by preparing paper and cloth-based Fe_1-Ni_1CoP@paper, Fe_1-Ni_1MoP@paper, Fe_1-Ni_1BP@cloth, and Fe_1-Ni_1WP@cloth electrodes, demonstrating the great potential of non-metallic substrates.

Furthermore, the strategic design of nanostructured catalysts is pivotal in boosting their stability. Specific formations such as nanowires, nanorods, nanosheets, or more intricate porous nanomaterials, have proven effective in enhancing material resilience against deformation and chemical degradation under conditions of high industrial current densities. For instance, Ma et al. developed nickel-cobalt phosphide nanowires demonstrating remarkable stability at industrial-scale current densities with only minimal reductions in current density after 100 continuous hours. Guo et al. explored a novel approach by integrating NiFe layered double hydroxide nanosheets with vertically aligned Mxene nanosheets, as illustrated in Figure 8c. This layered 3D electrode structure facilitated a significant enhancement in charge transfer rates through a pronounced synergistic effect

 doi:10.20944/preprints202405.0854.v1

among internal electrons, thereby considerably expediting the kinetics of the hydrogen evolution reaction (HER). Moreover, this innovative electrode showcased exceptional durability, maintaining stable operation for 400 hours.

Interestingly, combining 0D, 1D, and 2D nanostructures to form a 3D layered self-supporting electrode emerges as an effective strategy. Yu and colleagues opted for Cu nanowires, NiFe nanosheets, and Pt_3Ir alloy nanoparticles to fabricate a Cu NWs@NiFe-Pt_3Ir core-shell structure (Figure 8d). Notably, the forest-like structure of the Cu nanowires, even after undergoing a series of calcination and reduction treatments, retains its original configuration, which imparts exceptional stability to the catalyst. Post-cyclic polarization (CP) testing, the hierarchical structure of the catalyst remained intact, with Pt_3Ir alloy nanoparticles still evenly distributed over the NiFe nanosheets, and the distribution of Pt and Ir elements on the Pt_3Ir also remained uniform. The results indicate that this electrocatalyst exhibits an extraordinarily low overpotential of just 239 mV at a current density of 1000 mA cm^{-2} (Figure 8e). Even more impressively, after continuous operation at 500 mA cm^{-2} for seven days, the potential of the Cu NWs@NiFe-Pt_3Ir showed only minimal changes, demonstrating its remarkable durability (Figure 8f).

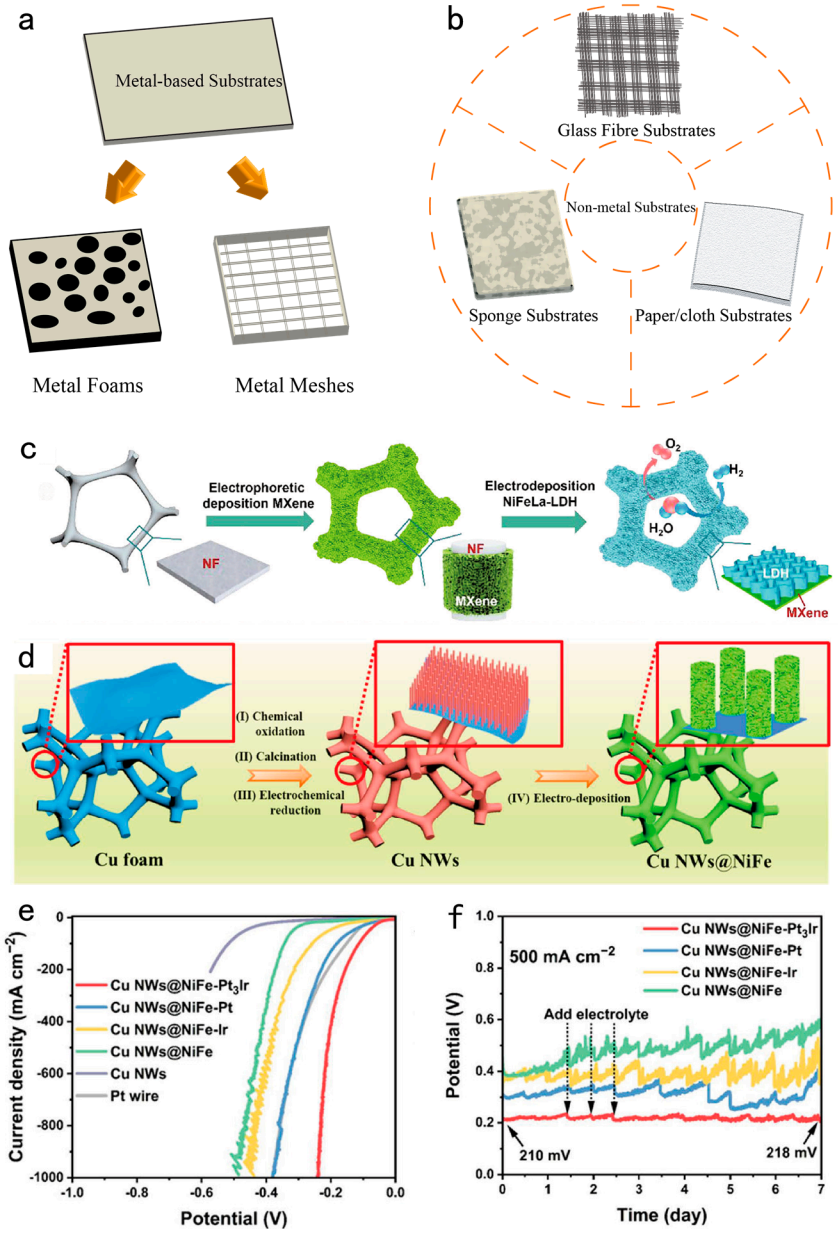

Figure 8. Schematics show self-supported substrates including **(a)** metal-based substrates, and **(b)** non-metal substrates. **(c)** The schematic illustration of the fabrication of NiFeLa-LDH/v-MXene/NF.

 doi:10.20944/preprints202405.0854.v1

Adapted with permission from [76], Copyright 2022 Elsevier. **(d)** Schematic illustration for the synthetic process of Cu NWs@NiFe. **(e)** LSV curves of the Cu NWs@NiFe-Pt_3Ir, Cu NWs@NiFe-Pt, Cu NWs@NiFe-Ir, Cu NWs@NiFe, Cu NWs, and Pt wire, respectively. **(f)** Chronopotentiometry curves of the Cu NWs@NiFe-Pt_3Ir, Cu NWs@NiFe-Pt, Cu NWs@NiFe-Ir, and Cu NWs@NiFe. Adapted with permission from [77], Copyright 2022 Elsevier.

4. Conclusions and Outlooks

Electrochemical water splitting is considered a promising pathway to advance the field of hydrogen energy research. The fabrication of efficient and robust catalysts in industrially relevant environments is essential for water splitting. In this review, we focus on challenges and design strategies for high current density water splitting electrocatalysts. In terms of challenges, catalytic activity, mass diffusion and catalyst stability are the three main challenges for electrocatalysts. To address these challenges, a number of catalyst design strategies are proposed. First, enhancement of the electrocatalyst active site activity and increase in the number of electrocatalyst active sites lead to improved charge transfer capability. Second, the detachment of bubbles can be effectively promoted by designing superwetting structures, thereby improving mass diffusion at high current densities. Third, self-supporting electrodes were designed to improve the long-term stability of the electrocatalysts. The HER performance of above-mentioned electrocatalysts is summarized in Table 1.

Table 1. Summary of some nano electrocatalysts for high-current-density HER.

Design strategy	Electrocatalyst	Electrolyte	Activity ($mV@mA\ cm^{-2}$)	Stability ($h@mA\ cm^{-2}$)	Ref.
Electronic structure modulation	Ce-CoP/Ni_3P	1 M KOH	225@1000	200@500	[60]
	Bi_2O_3-O_V	1 M KOH	310@300	/	[61]
	HSD-PtNi/NF	1 M KOH	63@1000	300@1000	[62]
	MnCo/NiSe/NF	1 M KOH	211.6@1000	150@500	[65]
	Am-Mo-$NiS_{0.5}Se_{0.5}$	1 M PBS	209@1000	/	[66]
	MoO_2@Ru	1 M KOH	131@1000	100@1000	[78]
	Pt/NiO_x-O_V	1 M KOH	≈180@500	100@1000	[79]
	Ru-$NiSe_2$	1 M KOH	180.8@1000	90@1000	[80]
	Ru-Ni_3N/NiO	1 M KOH	190@1000	1000@500	[81]
	Ru/Ni@C	1 M KOH	309@1000	100@1000	[82]
	Co/NC-HP@Si-NW	0.5M H_2SO_4	440@500	24@500	[83]
	MoS_2-P2	1 M KOH	332@500	240@500	[84]
Crystal phase modulation	MnO/CoP/NF	1 M KOH	259.5@1000	100@500	[85]
	Fe_2P/Co_2N	1 M KOH	131@500	40@500	[86]
	Mo_2N/Ni_3Mo_3N	1 M KOH	123@500	120@500	[87]
	$(Fe,Ni)_2P$@Ni_2P	1 M KOH	255@1000	120@1000	[88]
	RuCo@$Ru_{SA}Co_{SA}$-NMC	1 M KOH	291@1500	576@1000	[89]
	PtNiMg	1 M KOH	/	100@2000	[90]
Superwetting structure	Ni(OH)x/Ni_3S_2	1 M KOH	238@1000	1000@320	[70]
	NCP/PC	1 M KOH	145@1000	1000@1000	[73]
	MoNi/$NiMoO_x$	1 M KOH	139@1900	100@600	[91]
	HW-NiMoN/NF-2h	1 M KOH	107@1000	100@500	[92]

 doi:10.20944/preprints202405.0854.v1

	Pt-Ni@NiMoN/NF	1 M KOH	90@500	120@1000	[93]
Self-supported electrodes	Cu NWs@NiFe-Pt_3Ir	1 M KOH	239@1000	168@500	[77]
	FeCoCrCuOx@CF	1 M KOH	/	160@500	[94]
	NMFSOH	1 M KOH	200@1000	300@500	[95]
	$Fe_{0.01}$-Ni&$Ni_{0.2}Mo_{0.8}N$	1 M KOH	135@500	100@400	[96]
	NiFe-LDH@NiMo-H2@NF	1 M KOH	73@500	400@500	[97]
	IrNi-$FeNi_3$/NF	1 M KOH	288.8@1000	124@1000	[98]
	Ni_5P_4-Co_2P/NCF	1 M KOH	267@1000	100@250	[99]
	MnO_X/NiFeP/NF	1 M KOH	255@500	120@500	[100]

Despite significant progress in the development of efficient electrocatalysts for high-current-density water splitting, there is still a large gap between laboratory-scale studies and industrial-scale applications. Looking forward, many challenges are still urgent to be overcome.

(1) Scale-up production and synthesis of electrocatalysts: In high-current-density water splitting, although some excellent electrocatalysts exhibit good stability, they are complex to synthesize and difficult to scale up, limiting their use in commercial alkaline electrolyzers. These electrolyzers typically require large-area electrodes, which are difficult to meet with traditional laboratory-scale solvent heating and electrodeposition methods. To overcome these challenges, experimental designs need to consider the scalability of the synthesis methods, such as the integration of superior catalysts into the electrodes using commercial thermal spray processes, or secondary processing of commercial electrodes to enhance performance. In addition, the development of new synthesis techniques such as wet chemical methods and 3D printing is also seen as a powerful way to achieve scale-up. While pursuing technical feasibility, the economic and environmental impacts of the catalysts need to be considered to ensure the cost-effectiveness of the electrodes and the environmental sustainability of their production.

(2) Advances in in situ and operational characterization techniques: In electrocatalytic studies, phase characterization of catalysts is usually only possible in their stable final state, which limits our in-depth understanding of the micro-mechanisms of catalytic reactions. The development of in situ and operational characterization techniques is crucial for monitoring phase changes during catalysis, especially when it comes to unraveling the mechanism of HER. Although there are still current controversies regarding the mechanism of HER, for example, whether the hydrogen binding energy is the only determinant of activity, in situ techniques can help to resolve these controversies by providing direct evidence about the reaction intermediates. Therefore, the application of in situ and operational characterization techniques to practical electrochemical processes can not only observe the internal changes of catalysts, but also reveal the phase evolution process and the detailed reaction mechanism, offering the possibility of designing more efficient catalysts.

(3) The environmental adaptability of electrocatalysts: The adaptation of electrocatalysts under different electrolyte conditions is one of the central issues of great interest in the field of electrochemistry today. Although most studies have focused on the performance under alkaline conditions, their behavior under acidic and neutral environments has not been fully appreciated. Understanding the differences in the performance of electrocatalysts under different pH environments is crucial, not only for hydrogen energy technology and water utilization, but also for the study of other electrocatalytic reactions. In order to achieve this goal, extensive performance evaluations are needed, including electrocatalytic activity in acidic, neutral, and alkaline electrolytes as well as stability and efficiency tests under simulated industrial conditions. In addition, standardized catalyst test methods and seawater electrolysis components need to be developed in order to advance electrocatalyst technology towards practical applications. This will help ensure

 doi:10.20944/preprints202405.0854.v1

consistent and comparable evaluations and provide a solid foundation for future electrocatalyst design and optimization.

(4) Innovations in electrode design: The key to innovation in electrode design is to enhance the bonding between the catalyst and the substrate by optimizing the hydrophilic and hydrophobic properties of the electrode and introducing novel structures such as 3D self-supporting electrodes to enhance electrolysis efficiency and long-term stability. By adjusting the chemical composition and microstructure of the electrode surface, such as micro- or nano-scale roughness, we can significantly improve the hydrophilicity of the electrode, which helps to increase the contact with the aqueous electrolyte and facilitates ion transport. Meanwhile, the superhydrophobic design, such as through nano-arrays and layered structures, can reduce the adhesion of gas bubbles on the electrode surface and accelerate the gas emission, thus improving the gas transfer efficiency of the overall electrolysis process. In addition, optimal activity and stability can be achieved by optimizing the structure and composition of the electrocatalysts at the atomic, nano and micro scales. These multiscale design strategies not only improve the performance of electrodes, but also help to improve the matching of electrolyzer and electrodes, and promote the widespread adoption of electrolysis technology in industrial applications.

(5) Systematic study of temperature and pressure: An in-depth study of catalyst performance under different environmental conditions, especially taking into account temperature and pressure variations, is essential for optimizing electrocatalytic processes in industrial applications. In practice, catalysts undergo significant changes in active sites and structure under the influence of high temperatures and pressures, and these changes can significantly affect electrocatalytic performance and reaction kinetics. Therefore, by simulating these harsh industrial conditions and evaluating the catalysts, it can help us to gain a deeper understanding and improve the design and functionality of electrocatalysts to meet industrial standards and efficiency requirements.

Funding: This work was financially supported by the Natural Science Foundation of China (51902101), the Youth Natural Science Foundation of Hunan Province (2021JJ540044), the Natural Science Foundation of Jiangsu Province (BK20201381), and the Science Foundation of Nanjing University of Posts and Telecommunications (NY219144).

Institutional Review Board Statement: Not applicable.

Informed Consent Statement: Not applicable.

Data Availability Statement: Not applicable.

Conflicts of Interest: The authors declare no conflict of interest.

References

1. Wang, Y.; Chen, K.S.; Mishler, J.; Cho, S.C.; Adroher, X.C. A Review of Polymer Electrolyte Membrane Fuel Cells: Technology, Applications, and Needs on Fundamental Research. *Appl. Energy* **2011,** *88*, 981-1007.
2. Cortés, A.; Feijoo, G.; Chica, A.; Da Costa-Serra, J.F.; Moreira, M.T. Environmental Implications of Biohydrogen Based Energy Production from Steam Reforming of Alcoholic Waste. *Ind. Crops Prod.* **2019,** *138*.
3. Brennan, L.; Owende, P. Biofuels from Microalgae-a Review of Technologies for Production, Processing, and Extractions of Biofuels and Co-Products. *Renewable Sustainable Energy Rev.* **2010,** *14*, 557-577.
4. Siddiqui, O.; Dincer, I. A Well to Pump Life Cycle Environmental Impact Assessment of Some Hydrogen Production Routes. *Int. J. Hydrogen Energy* **2019,** *44*, 5773-5786.
5. Wen, Q.; Zhao, Y.; Liu, Y.; Li, H.; Zhai, T. Ultrahigh-Current-Density and Long-Term-Durability Electrocatalysts for Water Splitting. *Small* **2022,** *18*, 2104513.
6. Chen, Y.; Yu, J.; Jia, J.; Liu, F.; Zhang, Y.; Xiong, G.; Zhang, R.; Yang, R.; Sun, D.; Liu, H. Metallic Ni_3Mo_3N Porous Microrods with Abundant Catalytic Sites as Efficient Electrocatalyst for Large Current Density and Superstability of Hydrogen Evolution Reaction and Water Splitting. *Appl. Catal., B* **2020,** *272*, 118956.
7. Lv, X.; Wan, S.; Mou, T.; Han, X.; Zhang, Y.; Wang, Z.; Tao, X. Atomic-Level Surface Engineering of Nickel Phosphide Nanoarrays for Efficient Electrocatalytic Water Splitting at Large Current Density. *Adv. Funct. Mater.* **2023,** *33*, 2205161.

 doi:10.20944/preprints202405.0854.v1

8. Qian, G.; Chen, J.; Luo, L.; Yu, T.; Wang, Y.; Jiang, W.; Xu, Q.; Feng, S.; Yin, S. Industrially Promising Nanowire Heterostructure Catalyst for Enhancing Overall Water Splitting at Large Current Density. *ACS Sustainable Chem. Eng.* **2020,** *8*, 12063-12071.
9. Wu, T.; Xu, S.; Zhang, Z.; Luo, M.; Wang, R.; Tang, Y.; Wang, J.; Huang, F. Bimetal Modulation Stabilizing a Metallic Heterostructure for Efficient Overall Water Splitting at Large Current Density. *Adv. Sci. Lett.* **2022,** *9*, 2202750.
10. Wang, P.; Luo, Y.; Zhang, G.; Wu, M.; Chen, Z.; Sun, S.; Shi, Z. MnO_x-Decorated Nickel-Iron Phosphides Nanosheets: Interface Modifications for Robust Overall Water Splitting at Ultra-High Current Densities. *Small* **2022,** *18*, 2105803.
11. Zhang, Y.; Zheng, X.; Guo, X.; Zhang, J.; Yuan, A.; Du, Y.; Gao, F. Design of Modified MOFs Electrocatalysts for Water Splitting: High Current Density Operation and Long-Term Stability. *Appl. Catal., B* **2023**, 122891.
12. Wu, D.; Chen, D.; Zhu, J.; Mu, S. Ultralow Ru Incorporated Amorphous Cobalt-Based Oxides for High-Current-Density Overall Water Splitting in Alkaline and Seawater Media. *Small* **2021,** *17*, 2102777.
13. Wang, F.-L.; Li, X.-Y.; Dong, Y.-W.; Nan, J.; Sun, Y.-M.; Yu, H.-B.; Zhang, X.-Y.; Dong, B.; Chai, Y.-M. Strong Ion Interaction Inducing Ultrahigh Activity of NiCoP Nanowires for Overall Water Splitting at Large Current Density. *Appl. Surf. Sci.* **2022,** *589*, 152837.
14. Yan, F.; Wang, Y.; Li, K.; Zhu, C.; Gao, P.; Li, C.; Zhang, X.; Chen, Y. Highly Stable Three-Dimensional Porous Nickel-Iron Nitride Nanosheets for Full Water Splitting at High Current Densities. *Chem.–Eur. J.* **2017,** *23*, 10187-10194.
15. Jian, J.; Yuan, L.; Qi, H.; Sun, X.; Zhang, L.; Li, H.; Yuan, H.; Feng, S. Sn-Ni_3S_2 Ultrathin Nanosheets as Efficient Bifunctional Water-Splitting Catalysts with a Large Current Density and Low Overpotential. *ACS Appl. Mater. Interfaces* **2018,** *10*, 40568-40576.
16. Li, S.; Sirisomboonchai, S.; Yoshida, A.; An, X.; Hao, X.; Abudula, A.; Guan, G. Bifunctional CoNi/$CoFe_2O_4$/Ni Foam Electrodes for Efficient Overall Water Splitting at a High Current Density. *J. Mater. Chem. A* **2018,** *6*, 19221-19230.
17. Wen, Q.; Yang, K.; Huang, D.; Cheng, G.; Ai, X.; Liu, Y.; Fang, J.; Li, H.; Yu, L.; Zhai, T. Schottky Heterojunction Nanosheet Array Achieving High-Current-Density Oxygen Evolution for Industrial Water Splitting Electrolyzers. *Adv. Energy Mater.* **2021,** *11*, 2102353.
18. Yu, T.; Xu, Q.; Qian, G.; Chen, J.; Zhang, H.; Luo, L.; Yin, S. Amorphous CoO_x-Decorated Crystalline RuO_2 Nanosheets as Bifunctional Catalysts for Boosting Overall Water Splitting at Large Current Density. *ACS Sustainable Chem. Eng.* **2020,** *8*, 17520-17526.
19. Luo, Y.; Zhang, Z.; Yang, F.; Li, J.; Liu, Z.; Ren, W.; Zhang, S.; Liu, B. Stabilized Hydroxide-Mediated Nickel-Based Electrocatalysts for High-Current-Density Hydrogen Evolution in Alkaline Media. *Energy Environ. Sci.* **2021,** *14*, 4610-4619.
20. Choi, C.; Ashby, D.S.; Butts, D.M.; DeBlock, R.H.; Wei, Q.; Lau, J.; Dunn, B. Achieving High Energy Density and High Power Density with Pseudocapacitive Materials. *Nat. Rev. Mater.* **2020,** *5*, 5-19.
21. Liang, C.; Zou, P.; Nairan, A.; Zhang, Y.; Liu, J.; Liu, K.; Hu, S.; Kang, F.; Fan, H.J.; Yang, C. Exceptional Performance of Hierarchical Ni-Fe Oxyhydroxide@ NiFe Alloy Nanowire Array Electrocatalysts for Large Current Density Water Splitting. *Energy Environ. Sci.* **2020,** *13*, 86-95.
22. Sun, H.; Tian, C.; Fan, G.; Qi, J.; Liu, Z.; Yan, Z.; Cheng, F.; Chen, J.; Li, C.P.; Du, M. Boosting Activity on Co_4N Porous Nanosheet by Coupling CeO_2 for Efficient Electrochemical Overall Water Splitting at High Current Densities. *Adv. Funct. Mater.* **2020,** *30*, 1910596.
23. Xing, Z.; Liu, Q.; Asiri, A.M.; Sun, X. High-Efficiency Electrochemical Hydrogen Evolution Catalyzed by Tungsten Phosphide Submicroparticles. *ACS Catal.* **2015,** *5*, 145-149.
24. Zhang, X.-Y.; Zhu, Y.-R.; Chen, Y.; Dou, S.-Y.; Chen, X.-Y.; Dong, B.; Guo, B.-Y.; Liu, D.-P.; Liu, C.-G.; Chai, Y.-M. Hydrogen Evolution under Large-Current-Density Based on Fluorine-Doped Cobalt-Iron Phosphides. *Chem. Eng. J. (Lausanne)* **2020,** *399*, 125831.
25. Chai, S.; Zhang, G.; Li, G.; Zhang, Y. Industrial Hydrogen Production Technology and Development Status in China: A Review. *Clean Technol. Environ. Policy* **2021,** *23*, 1931-1946.
26. Zhang, X.-Y.; Yu, W.-L.; Zhao, J.; Dong, B.; Liu, C.-G.; Chai, Y.-M. Recent Development on Self-Supported Transition Metal-Based Catalysts for Water Electrolysis at Large Current Density. *Appl. Mater. Today* **2021,** *22*, 100913.
27. Li, S.; Li, E.; An, X.; Hao, X.; Jiang, Z.; Guan, G. Transition Metal-Based Catalysts for Electrochemical Water Splitting at High Current Density: Current Status and Perspectives. *Nanoscale* **2021,** *13*, 12788-12817.
28. Park, H.; Zhang, Y.; Lee, E.; Shankhari, P.; Fokwa, B.P. High-Current-Density HER Electrocatalysts: Graphene-Like Boron Layer and Tungsten as Key Ingredients in Metal Diborides. *ChemSusChem* **2019,** *12*, 3726-3731.
29. Jin, M.; Zhang, X.; Niu, S.; Wang, Q.; Huang, R.; Ling, R.; Huang, J.; Shi, R.; Amini, A.; Cheng, C. Strategies for Designing High-Performance Hydrogen Evolution Reaction Electrocatalysts at Large Current Densities above 1000 mA cm^{-2}. *ACS Nano* **2022,** *16*, 11577-11597.

30. Cao, D.; Zhang, Z.; Cui, Y.; Zhang, R.; Zhang, L.; Zeng, J.; Cheng, D. One-Step Approach for Constructing High-Density Single-Atom Catalysts toward Overall Water Splitting at Industrial Current Densities. *Angew. Chem.* **2023,** *135*, e202214259.
31. Qiu, Y.; Liu, S.; Wei, C.; Fan, J.; Yao, H.; Dai, L.; Wang, G.; Li, H.; Su, B.; Guo, X. Synergistic Effect between Platinum Single Atoms and Oxygen Vacancy in MoO_2 Boosting pH-Universal Hydrogen Evolution Reaction at Large Current Density. *Chem. Eng. J. (Lausanne)* **2022,** *427*, 131309.
32. Zhou, Q.; Liao, L.; Zhou, H.; Li, D.; Tang, D.; Yu, F. Innovative Strategies in Design of Transition Metal-Based Catalysts for Large-Current-Density Alkaline Water/Seawater Electrolysis. *Mater. Today Phys.* **2022,** *26*, 100727.
33. Xu, Y.; Wang, C.; Huang, Y.; Fu, J. Recent Advances in Electrocatalysts for Neutral and Large-Current-Density Water Electrolysis. *Nano Energy* **2021,** *80*, 105545.
34. Endrődi, B.; Kecsenovity, E.; Samu, A.; Halmágyi, T.; Rojas-Carbonell, S.; Wang, L.; Yan, Y.; Janáky, C. High Carbonate Ion Conductance of a Robust Piperion Membrane Allows Industrial Current Density and Conversion in a Zero-Gap Carbon Dioxide Electrolyzer Cell. *Energy Environ. Sci.* **2020,** *13*, 4098-4105.
35. Hu, Y.; Chen, W.; Lei, T.; Zhou, B.; Jiao, Y.; Yan, Y.; Du, X.; Huang, J.; Wu, C.; Wang, X. Carbon Quantum Dots-Modified Interfacial Interactions and Ion Conductivity for Enhanced High Current Density Performance in Lithium-Sulfur Batteries. *Adv. Energy Mater.* **2019,** *9*, 1802955.
36. Yu, L.; Mishra, I.K.; Xie, Y.; Zhou, H.; Sun, J.; Zhou, J.; Ni, Y.; Luo, D.; Yu, F.; Yu, Y. Ternary $Ni_{2(1-X)}Mo_{2x}P$ Nanowire Arrays toward Efficient and Stable Hydrogen Evolution Electrocatalysis under Large-Current-Density. *Nano Energy* **2018,** *53*, 492-500.
37. Yao, Y.; Zhu, Y.; Pan, C.; Wang, C.; Hu, S.; Xiao, W.; Chi, X.; Fang, Y.; Yang, J.; Deng, H. Interfacial Sp C-O-Mo Hybridization Originated High-Current Density Hydrogen Evolution. *J. Am. Chem. Soc.* **2021,** *143*, 8720-8730.
38. Friedl, J.; Bauer, C.M.; Rinaldi, A.; Stimming, U. Electron Transfer Kinetics of the Vo_{2+}/Vo_2^+-Reaction on Multi-Walled Carbon Nanotubes. *Carbon* **2013,** *63*, 228-239.
39. Wu, Z.; Fang, B.; Wang, Z.; Wang, C.; Liu, Z.; Liu, F.; Wang, W.; Alfantazi, A.; Wang, D.; Wilkinson, D.P. MoS_2 Nanosheets: A Designed Structure with High Active Site Density for the Hydrogen Evolution Reaction. *ACS Catal.* **2013,** *3*, 2101-2107.
40. Li, Q.; Chen, C.; Luo, W.; Yu, X.; Chang, Z.; Kong, F.; Zhu, L.; Huang, Y.; Tian, H.; Cui, X. In Situ Active Site Refreshing of Electro-Catalytic Materials for Ultra-Durable Hydrogen Evolution at Elevated Current Density. *Adv. Energy Mater.* **2024**, 2304099.
41. Cheng, F.; Peng, X.; Hu, L.; Yang, B.; Li, Z.; Dong, C.-L.; Chen, J.-L.; Hsu, L.-C.; Lei, L.; Zheng, Q. Accelerated Water Activation and Stabilized Metal-Organic Framework Via Constructing Triangular Active-Regions for Ampere-Level Current Density Hydrogen Production. *Nat. Commun.* **2022,** *13*, 6486.
42. Xie, J.; Zhang, H.; Li, S.; Wang, R.; Sun, X.; Zhou, M.; Zhou, J.; Lou, X.W.; Xie, Y. Defect-Rich MoS_2 Ultrathin Nanosheets with Additional Active Edge Sites for Enhanced Electrocatalytic Hydrogen Evolution. *Adv. Mater.* **2013**, 5807-5813.
43. Ebrahimi, F.; Ahmed, Z. The Effect of Current Density on Properties of Electrodeposited Nanocrystalline Nickel. *J. Appl. Electrochem.* **2003,** *33*, 733-739.
44. Jiang, J.-Q.; Graham, N.; André, C.; Kelsall, G.H.; Brandon, N. Laboratory Study of Electro-Coagulation-Flotation for Water Treatment. *Water Res.* **2002,** *36*, 4064-4078.
45. Olesen, A.C.; Frensch, S.H.; Kær, S.K. Towards Uniformly Distributed Heat, Mass and Charge: A Flow Field Design Study for High Pressure and High Current Density Operation of Pem Electrolysis Cells. *Electrochim. Acta* **2019,** *293*, 476-495.
46. Xiao, C.; Li, Y.; Lu, X.; Zhao, C. Bifunctional Porous NiFe/$NiCo_2O_4$/Ni Foam Electrodes with Triple Hierarchy and Double Synergies for Efficient Whole Cell Water Splitting. *Adv. Funct. Mater.* **2016,** *26*, 3515-3523.
47. Yang, Y.; Li, J.; Yang, Y.; Lan, L.; Liu, R.; Fu, Q.; Zhang, L.; Liao, Q.; Zhu, X. Gradient Porous Electrode-Inducing Bubble Splitting for Highly Efficient Hydrogen Evolution. *Appl. Energy* **2022,** *307*, 118278.
48. Bae, M.; Kang, Y.; Lee, D.W.; Jeon, D.; Ryu, J. Superaerophobic Polyethyleneimine Hydrogels for Improving Electrochemical Hydrogen Production by Promoting Bubble Detachment. *Adv. Energy Mater.* **2022,** *12*, 2201452.
49. Kou, T.; Wang, S.; Shi, R.; Zhang, T.; Chiovoloni, S.; Lu, J.Q.; Chen, W.; Worsley, M.A.; Wood, B.C.; Baker, S.E. Periodic Porous 3D Electrodes Mitigate Gas Bubble Traffic During Alkaline Water Electrolysis at High Current Densities. *Adv. Energy Mater.* **2020,** *10*, 2002955.
50. Li, Y.; Yang, G.; Yu, S.; Kang, Z.; Mo, J.; Han, B.; Talley, D.A.; Zhang, F.-Y. In-Situ Investigation and Modeling of Electrochemical Reactions with Simultaneous Oxygen and Hydrogen Microbubble Evolutions in Water Electrolysis. *Int. J. Hydrogen Energy* **2019,** *44*, 28283-28293.
51. Park, S.; Liu, L.; Demirkır, Ç.; van der Heijden, O.; Lohse, D.; Krug, D.; Koper, M.T. Solutal Marangoni Effect Determines Bubble Dynamics During Electrocatalytic Hydrogen Evolution. *Nature chemistry* **2023,** *15*, 1532-1540.

 doi:10.20944/preprints202405.0854.v1

52. Li, Y.; Zhang, H.; Xu, T.; Lu, Z.; Wu, X.; Wan, P.; Sun, X.; Jiang, L. Under-Water Superaerophobic Pine-Shaped Pt Nanoarray Electrode for Ultrahigh-Performance Hydrogen Evolution. *Adv. Funct. Mater.* **2015,** *25*, 1737-1744.
53. Shang, L.; Zhao, Y.; Kong, X.-Y.; Shi, R.; Waterhouse, G.I.; Wen, L.; Zhang, T. Underwater Superaerophobic Ni Nanoparticle-Decorated Nickel-Molybdenum Nitride Nanowire Arrays for Hydrogen Evolution in Neutral Media. *Nano Energy* **2020,** *78*, 105375.
54. Luo, Y.; Zhang, Z.; Chhowalla, M.; Liu, B. Recent Advances in Design of Electrocatalysts for High-Current-Density Water Splitting. *Adv. Mater.* **2022,** *34*, 2108133.
55. Wu, T.; Song, E.; Zhang, S.; Luo, M.; Zhao, C.; Zhao, W.; Liu, J.; Huang, F. Engineering Metallic Heterostructure Based on Ni_3N and 2M-MoS_2 for Alkaline Water Electrolysis with Industry-Compatible Current Density and Stability. *Adv. Mater.* **2022,** *34*, 2108505.
56. Qian, G.; Chen, J.; Yu, T.; Luo, L.; Yin, S. N-Doped Graphene-Decorated NiCo Alloy Coupled with Mesoporous NiCoMoO Nano-Sheet Heterojunction for Enhanced Water Electrolysis Activity at High Current Density. *Nano Micro Lett.* **2021,** *13*, 1-13.
57. Lu, X.; Zhao, C. Electrodeposition of Hierarchically Structured Three-Dimensional Nickel-Iron Electrodes for Efficient Oxygen Evolution at High Current Densities. *Nat. Commun.* **2015,** *6*, 1-7.
58. Raja, D.S.; Lin, H.-W.; Lu, S.-Y. Synergistically Well-Mixed Mofs Grown on Nickel Foam as Highly Efficient Durable Bifunctional Electrocatalysts for Overall Water Splitting at High Current Densities. *Nano Energy* **2019,** *57*, 1-13.
59. Jin, H.; Liu, X.; Chen, S.; Vasileff, A.; Li, L.; Jiao, Y.; Song, L.; Zheng, Y.; Qiao, S.-Z. Heteroatom-Doped Transition Metal Electrocatalysts for Hydrogen Evolution Reaction. *ACS Energy Lett.* **2019,** *4*, 805-810.
60. Zhang, F.; Wang, X.; Han, W.; Qian, Y.; Qiu, L.; He, Y.; Lei, L.; Zhang, X. The Synergistic Activation of Ce-Doping and CoP/Ni_3P Hybrid Interaction for Efficient Water Splitting at Large-Current-Density. *Adv. Funct. Mater.* **2022,** *33*.
61. Wu, Z.; Liao, T.; Wang, S.; Mudiyanselage, J.A.; Micallef, A.S.; Li, W.; O'Mullane, A.P.; Yang, J.; Luo, W.; Ostrikov, K.; Gu, Y.; Sun, Z. Conversion of Catalytically Inert 2D Bismuth Oxide Nanosheets for Effective Electrochemical Hydrogen Evolution Reaction Catalysis Via Oxygen Vacancy Concentration Modulation. *Nano Micro Lett.* **2022,** *14*.
62. Zhou, M.; Cheng, C.; Dong, C.; Xiao, L.; Zhao, Y.; Liu, Z.; Zhao, X.; Sasaki, K.; Cheng, H.; Du, X.; Yang, J. Dislocation Network-Boosted PtNi Nanocatalysts Welded on Nickel Foam for Efficient and Durable Hydrogen Evolution at Ultrahigh Current Densities. *Adv. Energy Mater.* **2022,** *13*.
63. Yang, W.; Cheng, P.; Li, Z.; Lin, Y.; Li, M.; Zi, J.; Shi, H.; Li, G.; Lian, Z.; Li, H. Tuning the Cobalt-Platinum Alloy Regulating Single-Atom Platinum for Highly Efficient Hydrogen Evolution Reaction. *Adv. Funct. Mater.* **2022,** *32*.
64. Liu, H.; Qin, H.; Kang, J.; Ma, L.; Chen, G.; Huang, Q.; Zhang, Z.; Liu, E.; Lu, H.; Li, J.; Zhao, N. A Freestanding Nanoporous Nicofemomn High-Entropy Alloy as an Efficient Electrocatalyst for Rapid Water Splitting. *Chem. Eng. J. (Lausanne)* **2022,** *435*.
65. Andaveh, R.; Sabour Rouhaghdam, A.; Ai, J.; Maleki, M.; Wang, K.; Seif, A.; Barati Darband, G.; Li, J. Boosting the Electrocatalytic Activity of NiSe by Introducing MnCo as an Efficient Heterostructured Electrocatalyst for Large-Current-Density Alkaline Seawater Splitting. *Appl. Catal., B* **2023,** *325*.
66. Wang, Y.; Li, X.; Huang, Z.; Wang, H.; Chen, Z.; Zhang, J.; Zheng, X.; Deng, Y.; Hu, W. Amorphous Mo-Doped $NiS_{0.5}Se_{0.5}$ Nanosheets@Crystalline $NiS_{0.5}Se_{0.5}$Nanorods for High Current-Density Electrocatalytic Water Splitting in Neutral Media. *Angew. Chem. Int. Ed.* **2023,** *62*.
67. Zeng, C.; Zhang, J.; Jin, Y.; Ren, D.; Li, L.; Zhou, K.; Zhang, Q.; Liu, J.; Han, C.; Wang, H. Accelerated Mass/Electron Transfer by Self-Supporting Ni_2P@Cu_3P Heterostructure Array to Boost Alkaline Hydrogen Evolution at High Current Density. *Fuel* **2023,** *350*.
68. Chen, W.; Wei, W.; Li, F.; Wang, Y.; Liu, M.; Dong, S.; Cui, J.; Zhang, Y.; Wang, R.; Ostrikov, K.; Zang, S.Q. Tunable Built-in Electric Field in Ru Nanoclusters-Based Electrocatalyst Boosts Water Splitting and Simulated Seawater Electrolysis. *Adv. Funct. Mater.* **2023**.
69. Chen, J.; Luo, X.; Zhang, H.; Liang, X.; Xiao, K.; Ouyang, T.; Dan, M.; Liu, Z.-Q. Constructing Superhydrophilic Coru-LDH/PaNi Nanowires with Optimized Electronic Structure for Hydrogen Evolution Reaction. *Electrochim. Acta* **2023,** *439*.
70. He, W.; Zhang, R.; Cao, D.; Li, Y.; Zhang, J.; Hao, Q.; Liu, H.; Zhao, J.; Xin, H.L. Super-Hydrophilic Microporous Ni(OH)x/Ni_3S_2 Heterostructure Electrocatalyst for Large-Current-Density Hydrogen Evolution. *Small* **2022,** *19*.
71. Zhang, C.; X, Z.; H,N.; T, Y.; Kallio, T.; Y, C.; Lei J, L. Superaerophilic/Superaerophobic Cooperative Electrode for Efficient Hydrogen Evolution Reaction Via Enhanced Mass Transfer. *Sci. Adv.* **2023**, eadd6978.
72. Zhou, Q.; Xu, C.; Hou, J.; Ma, W.; Jian, T.; Yan, S.; Liu, H. Duplex Interpenetrating-Phase Fenizn and $FeNi_3$ Heterostructure with Low-Gibbs Free Energy Interface Coupling for Highly Efficient Overall Water Splitting. *Nano Micro Lett.* **2023,** *15*.

 doi:10.20944/preprints202405.0854.v1

73. Liang, J.; Cai, Z.; Li, Z.; Yao, Y.; Luo, Y.; Sun, S.; Zheng, D.; Liu, Q.; Sun, X.; Tang, B. Efficient Bubble/Precipitate Traffic Enables Stable Seawater Reduction Electrocatalysis at Industrial-Level Current Densities. *Nat. Commun.* **2024,** *15*.
74. Yan, S.; Chen, X.; Li, W.; Zhong, M.; Xu, J.; Xu, M.; Wang, C.; Pinna, N.; Lu, X. Highly Active and Stable Alkaline Hydrogen Evolution Electrocatalyst Based on Ir-Incorporated Partially Oxidized Ru Aerogel under Industrial-Level Current Density. *Adv. Sci. Lett.* **2023,** *11*.
75. Yang, C.; Zhong, W.; Shen, K.; Zhang, Q.; Zhao, R.; Xiang, H.; Wu, J.; Li, X.; Yang, N. Electrochemically Reconstructed Cu-FeOOH/Fe_3O_4 Catalyst for Efficient Hydrogen Evolution in Alkaline Media. *Adv. Energy Mater.* **2022,** *12*.
76. Yu, M.; Zheng, J.; Guo, M. La-Doped NiFe-LDH Coupled with Hierarchical Vertically Aligned Mxene Frameworks for Efficient Overall Water Splitting. *Journal of Energy Chemistry* **2022,** *70*, 472-479.
77. Ni, Z.; Luo, C.; Cheng, B.; Kuang, P.; Li, Y.; Yu, J. Construction of Hierarchical and Self-Supported NiFe-Pt_3Ir Electrode for Hydrogen Production with Industrial Current Density. *Appl. Catal., B* **2023,** *321*.
78. Zhang, Y.; Ma, C.; Zhu, X.; Qu, K.; Shi, P.; Song, L.; Wang, J.; Lu, Q.; Wang, A.L. Hetero-Interface Manipulation in MoO_x@Ru to Evoke Industrial Hydrogen Production Performance with Current Density of 4000 mA cm^{-2}. *Adv. Energy Mater.* **2023,** *13*.
79. Wang, K.; Wang, S.; Hui, K.S.; Li, J.; Zha, C.; Dinh, D.A.; Shao, Z.; Yan, B.; Tang, Z.; Hui, K.N. Dense Platinum/Nickel Oxide Heterointerfaces with Abundant Oxygen Vacancies Enable Ampere-Level Current Density Ultrastable Hydrogen Evolution in Alkaline. *Adv. Funct. Mater.* **2022,** *33*.
80. Bai, Y.; Zhang, H.; Lu, X.; Wang, L.; Zou, Y.; Miao, J.; Qiao, M.; Tang, Y.; Zhu, D. Self-Supported Ru-Incorporated $NiSe_2$ for Ampere-Level Current Density Hydrogen Evolution. *Chemistry A European Journal* **2023,** *29*.
81. Liu, R.; Sun, M.; Liu, X.; Lv, Z.; Yu, X.; Wang, J.; Liu, Y.; Li, L.; Feng, X.; Yang, W.; Huang, B.; Wang, B. Enhanced Metal-Support Interactions Boost the Electrocatalytic Water Splitting of Supported Ruthenium Nanoparticles on a Ni_3N/NiO Heterojunction at Industrial Current Density. *Angew. Chem. Int. Ed.* **2023,** *62*.
82. Wang, L.; Liu, Y.; Chen, Z.; Dai, Q.; Dong, C.-L.; Yang, B.; Li, Z.; Hu, X.; Lei, L.; Hou, Y. Theory-Guided Design of Electron-Deficient Ruthenium Cluster for Ampere-Level Current Density Electrochemical Hydrogen Evolution. *Nano Energy* **2023,** *115*.
83. Yang, T.; Chen, Z.; Wang, Y.; Huang, H.; Yin, K.; Liao, F.; Liu, Y.; Kang, Z. In Situ Insertion of Silicon Nanowires into Hollow Porous Co/NC Polyhedra Enabling Large-Current-Density Hydrogen Evolution Electrocatalysis. *Small* **2023**.
84. Shi, Y.; Zhang, D.; Miao, H.; Wu, X.; Wang, Z.; Zhan, T.; Lai, J.; Wang, L. Amorphous/2H-MoS_2 Nanoflowers with P Doping and S Vacancies to Achieve Efficient pH-Universal Hydrogen Evolution at High Current Density. *Sci. China Chem.* **2022,** *65*, 1829-1837.
85. Dong, Y.; Deng, Z.; Zhang, H.; Liu, G.; Wang, X. A Highly Active and Durable Hierarchical Electrocatalyst for Large-Current-Density Water Splitting. *Nano Lett.* **2023,** *23*, 9087-9095.
86. Zhou, X.; Mo, Y.; Yu, F.; Liao, L.; Yong, X.; Zhang, F.; Li, D.; Zhou, Q.; Sheng, T.; Zhou, H. Engineering Active Iron Sites on Nanoporous Bimetal Phosphide/Nitride Heterostructure Array Enabling Robust Overall Water Splitting. *Adv. Funct. Mater.* **2022,** *33*.
87. Zhu, Z.; Luo, L.; He, Y.; Mushtaq, M.; Li, J.; Yang, H.; Khanam, Z.; Qu, J.; Wang, Z.; Balogun, M.S. High-Performance Alkaline Freshwater and Seawater Hydrogen Catalysis by Sword-Head Structured Mo_2N-Ni_3Mo_3N Tunable Interstitial Compound Electrocatalysts. *Adv. Funct. Mater.* **2023**.
88. Li, Y.; Yu, X.; Gao, J.; Ma, Y. Structural and Electronic Modulation of $(Fe,Ni)_2P$@Ni_2P Heterostructure for Efficient Overall Water Splitting at High Current Density. *Chem. Eng. J. (Lausanne)* **2023,** *470*.
89. Wang, X.; Yao, H.; Zhang, C.; Li, C.; Tong, K.; Gu, M.; Cao, Z.; Huang, M.; Jiang, H. Double-Tuned RuCo Dual Metal Single Atoms and Nanoalloy with Synchronously Expedited Volmer/Tafel Kinetics for Effective and Ultrastable Ampere-Level Current Density Hydrogen Production. *Adv. Funct. Mater.* **2023,** *33*.
90. Zheng, Y.; Shang, P.; Pei, F.; Ma, G.; Ye, Z.; Peng, X.; Li, D. Achieving an Efficient Hydrogen Evolution Reaction with a Bicontinuous Nanoporous Ptnimg Alloy of Ultralow Noble-Metal Content at an Ultrawide Range of Current Densities. *Chem. Eng. J. (Lausanne)* **2022,** *433*.
91. Shi, X.; Zheng, X.; Wang, H.; Zhang, H.; Qin, M.; Lin, B.; Qi, M.; Mao, S.; Ning, H.; Yang, R.; Xi, L.; Wang, Y. Hierarchical Crystalline/Amorphous Heterostructure MoNi/NiMoO_x for Electrochemical Hydrogen Evolution with Industry-Level Activity and Stability. *Adv. Funct. Mater.* **2023,** *33*.
92. Ning, M.; Wang, Y.; Wu, L.; Yang, L.; Chen, Z.; Song, S.; Yao, Y.; Bao, J.; Chen, S.; Ren, Z. Hierarchical Interconnected NiMoN with Large Specific Surface Area and High Mechanical Strength for Efficient and Stable Alkaline Water/Seawater Hydrogen Evolution. *Nano Micro Lett.* **2023,** *15*.
93. Hu, H.; Zhang, Z.; Zhang, Y.; Thomas, T.; Du, H.; Huang, K.; Attfield, J.P.; Yang, M. An Ultra-Low Pt Metal Nitride Electrocatalyst for Sustainable Seawater Hydrogen Production. *Energy Environ. Sci.* **2023,** *16*, 4584-4592.

94. Liu, C.; Feng, J.; Zhou, P.; Liu, D.; Qiao, L.; Liu, D.; Cao, Y.; Su, S.-C.; Liu, H.; Pan, H. Multi-Metal Interaction Boosts Reconstructed FeCoCrCuO$_x$@CF toward Efficient Alkaline Water Electrolysis under Large Current Density. *Chem. Eng. J. (Lausanne)* **2023,** *476*.
95. Fang, P.; Zhu, M.; Liu, J.; Zhu, Z.; Hu, J.; Xu, X. Making Ternary-Metal Hydroxysulfide Catalyst Via Cathodic Reconstruction with Ion Regulation for Industrial-Level Hydrogen Generation. *Adv. Energy Mater.* **2023,** *13*.
96. Ning, M.; Zhang, F.; Wu, L.; Xing, X.; Wang, D.; Song, S.; Zhou, Q.; Yu, L.; Bao, J.; Chen, S.; Ren, Z. Boosting Efficient Alkaline Fresh Water and Seawater Electrolysis Via Electrochemical Reconstruction. *Energy Environ. Sci.* **2022,** *15*, 3945-3957.
97. Zhang, Y.; Feng, B.; Yan, M.; Shen, Z.; Chen, Y.; Tian, J.; Xu, F.; Chen, G.; Wang, X.; Yang, L.; Wu, Q.; Hu, Z. Self-Supported NiFe-LDH Nanosheets on NiMo-Based Nanorods as High-Performance Bifunctional Electrocatalysts for Overall Water Splitting at Industrial-Level Current Densities. *Nano Research* **2023**.
98. Wang, Y.; Qian, G.; Xu, Q.; Zhang, H.; Shen, F.; Luo, L.; Yin, S. Industrially Promising IrNi-FeNi$_3$ Hybrid Nanosheets for Overall Water Splitting Catalysis at Large Current Density. *Appl. Catal., B* **2021,** *286*, 119881.
99. Chen, Y.; Chen, J.; Bai, K.; Xiao, Z.; Fan, S. A Flow-through Electrode for Hydrogen Production from Water Splitting by Mitigating Bubble Induced Overpotential. *J. Power Sources* **2023,** *561*, 232733.
100. Ning, S.; Wu, Q.; Zhu, Y.; Liu, S.; Zhou, W.; Mi, L.; Zhou, K.; Zhao, D.; Zhang, X.; Wang, N. N-Doped Carbon Nanowire Array Confined Cobalt Phosphides as Efficient Bifunctional Electrocatalysts for Water Splitting. *Inorg. Chem. Front.* **2023,** *10*, 2145-2153.